Journal of Environmental Radioactivity 270 (2023) 107291

Contents lists available at ScienceDirect

Journal of Environmental Radioactivity

journal homepage: www.elsevier.com/locate/jenvrad

Distribution and impacts of contamination by natural and artificial radionuclides in attic dust and urban soil samples from a former industrial Hungarian city: A case study from Salgótarján

Davaakhuu Tserendorj [a,g], Katalin Zsuzsanna Szabó [b], Péter Völgyesi [b], Tam Cong Nguyen [b], István Gábor Hatvani [c,d], Noémi Buczkó [e], Gorkhmaz Abbaszade [a], Nelson Salazar-Yanez [a], Csaba Szabó [a,f,*]

[a] Lithosphere Fluid Research Laboratory, Institute of Geography and Earth Sciences, Eötvös Loránd University, Pázmány Péter sétány 1/C, 1117, Budapest, Hungary
[b] Nuclear Security Department, HUN-REN Centre for Energy Research, Konkoly-Thege Miklós út 29-33, 1121, Budapest, Hungary
[c] Institute for Geological and Geochemical Research, HUN-REN Research Centre for Astronomy and Earth Sciences, Eötvös Loránd Research Network (ELKH), Budaörsi út 45, 1112, Budapest, Hungary
[d] CSFK, MTA Centre of Excellence, Konkoly Thege Miklós út 15-17, H-1121, Budapest, Hungary
[e] Nuclear Analysis and Radiography Department, HUN-REN Centre for Energy Research, Konkoly-Thege Miklós út 29-33, 1121, Budapest, Hungary
[f] Institute of Earth Physics and Space Science, HUN-REN, Csatkai E. u. 6-8, 9400, Sopron, Hungary
[g] Centre for Ecological Research Institute of Aquatic Ecology, Karolina út 29, 1113, Budapest, Hungary

ARTICLE INFO

Handling Editor: Dr S.C. Sheppard

Keywords:
Radionuclides
Attic dust
Urban soil
Coal-fired power plant
Northern Hungary

ABSTRACT

Primordial radionuclides can be found in all environmental compartments. Since coal-fired power plants (CFPP) can be a source of additional radionuclide contamination because coal contains natural radioactive isotopes such as ^{238}U (^{226}Ra) and ^{232}Th. This study investigated the impact of such possible radionuclide contamination from former heavy industrial activities, namely a former local coal-fired power plant, in urban soils and attic dust in Salgótarján, Hungary. Even today, industrial by-products, e.g., coal ash, in this city represent significant threat to its residents. A total of 36 attic dust samples (family houses, kindergartens, churches and blockhouses) were collected and 19 urban soil samples (playgrounds, kindergartens, parks and others) were selected no further than 500 m from the corresponding attic dust sampling sites. Additionally, a coal ash and a brown forest soil sample were also collected to differentiate between the anthropogenic and geogenic sources in the residential area. The sampled houses, built between 1890 and 1990, are considered to be representative sampling sites for long-term accumulations of attic dust. The mean values of the total U, Th and Cs (mg kg^{-1}) concentrations as well as those of K (m/m %) in attic dust and urban soil samples are 2.4, 3.6, 1.7 and 0.6 and 1.1, 4.4, 1.2 and 0.3, respectively, measured using ICP-MS. The mean activity concentrations of ^{226}Ra, ^{232}Th, ^{40}K and ^{137}Cs in attic dust and urban soil samples are 43.3, 34.0, 534.4 and 88.5 and 25.1, 32.8, 386.4 and 5.6 Bq kg^{-1}, respectively, by using a low-background iron chamber with a well-type HPGe and a n-type coaxial HPGe detector.

The elemental compositions (U, Th) and activity concentrations (^{226}Ra, ^{232}Th) along with their abundances in coal ash from the CFPP increase in both studied media as the distance of the sampling sites from the CFPP decreases. Two outlier attic dust samples in particular show significantly high activity concentrations of ^{226}Ra: 145 and 143, of ^{232}Th: 83 and 94 Bq kg^{-1}, which can be considered as a proxy of unweathered coal ash. The calculated total absorbed gamma dose rate (*D*) and annual effective dose (*E*) received from urban soils indicate that the presence of the CFPP, coal ash cone and slag dumps does not cause an increase in the level of background radiation in Salgótarján. However, the concentrations of the studied radionuclides are much higher (except for ^{232}Th) and exhibit higher degree of variability in the samples of attic dustthan in those of urban soils. The study suggests that attic dust preserves the undisturbed 'fingerprints' of long-term atmospheric deposition thanks to its chemical and physical properties unlike urban soil.

* Corresponding author. Lithosphere Fluid Research Laboratory, Institute of Geography and Earth Sciences, Eötvös Loránd University, Pázmány Péter sétány 1/C, 1117, Budapest, Hungary.
E-mail address: csaba.szabo@ttk.elte.hu (C. Szabó).

https://doi.org/10.1016/j.jenvrad.2023.107291
Received 23 March 2023; Received in revised form 17 August 2023; Accepted 28 August 2023
Available online 6 October 2023

1. Introduction

Radioactivity has become a major concern over the years because of its association with public health (UNSCEAR, 2010). Primordial radionuclides (^{238}U(^{226}Ra), ^{232}Th and ^{40}K) are present to various degrees in all environmental spheres as naturally occurring radioactive materials (NORMs). Human interventions, e.g., coal mining and operarion of coal-fired power plants, utilize, recover and dispose of these materials, thereby creating technologically enhanced naturally occurring radioactive materials (TENORMs) which can increase levels of radiation exposure (EPA, 2006). Furthermore, artificial radionuclides have been released into the atmosphere mostly as a result of nuclear weapons testing from the 1940's to 1980's and major nuclear accidents (Chernobyl, 1986 and Fukushima, 2011; UNSCEAR, 2010). Studies on environmental liability, such as those concerning contaminated sites and radioactive waste depository, provide valuable knowledge of radiation risk assessments associated with exposure and dose (Ahmad et al., 2019).

Since the 1960's, numerous studies from around the world such as from Poland, China and Brazil have been proposed focusing on contamination in the vicinity of coal-fired power plants (CFPP) (e.g., Bem et al., 2002; Charro et al., 2013a, b; Eisenbud and Petrow, 1964; Flues et al., 2002; Lu et al., 2012; Papaefthymiou et al., 2013; Tanić et al., 2016). Furthermore, several studies on the impact of radionuclides on urban soils in the vicinity of a coal-fired power plant in the town of Ajka (Hungary) have been carried out (Papp et al., 2002; Papp and Dezső, 2003; Zacháry et al., 2015) following the usage of local U-rich brown coal (Szabó, 1992). Most of these studies measured the radioactivity of surface soils in the vicinity of the local CFPP.

During coal combustion, natural radionuclides concentrate in the residual by-products, e.g. coal ash, resulting in activity concentrations up to ten times greater than those in burnt coal (IAEA, 2003). A proportion of this by-product (<100 μm grain size fraction) can easily be emitted into the atmosphere from slag dumps, from where people are exposed to through several transfer pathways in the biosphere (UNSCEAR, 2010). Furthermore, slag dumps are potentially risky for humans since they can increase natural background radiation levels. The particles emitted from CFPP are capable of getting into dwellings, e.g., through open windows, cracks and vents, as well as being deposited inside, especially in undisturbed attics as attic dust. Cizdziel and Hodge (2000) concluded that undisturbed attics may act as archives of atmospheric dust and should be researched by those interested in the accumulation of atmospheric dust and/or in reconstructing exposure histories.

Undisturbed archived attic dust as a long-term pollutant has been used to monitor potentially toxic elements, e.g., Pb, Cd, As (Balabanova et al., 2011, 2017; Cizdziel and Hodge, 2000; Davis and Gulson, 2005; Gosar et al., 2006; Ilacqua et al., 2003; Painecur et al., 2022; Sajn, 2005; Völgyesi et al., 2014a, 2014b) and polycyclic aromatic hydrocarbons (Coronas et al., 2013; Wheeler et al., 2020) that are thought to have been predominantly emitted from contamination sources into the ambient environment. The analyses of radionuclides, e.g., ^{137}Cs and ^{239}Pu (Cizdziel et al., 1998, 1999; Tserendorj et al., 2022a) have demonstrated that attic dust accumulates and preserves valuable information about the environment since it was only subjected to minor physical and chemical alterations (Cizdziel and Hodge, 2000; Lioy et al., 2002). Additionally, attic dust should also be regarded as a risk to human health, particularly in areas where long-term pollution processes are known to occur (Gabersek et al., 2022). However, since natural radionuclides in attic dust have not been studied at all, it is necessary to estimate whether attic dust is a radiological concern over decades, providing valuable radioactivity data compared to urban soils, which are considered as disturbed (Richard et al., 2019) materials when compared to attic dust.

Studies on the distribution of radionuclides in urban soils are important in terms of human health and well-being. Given that urban areas, covered by soil, like parks and playgrounds are where residents spend significant proportion of their recreation time, their investigation is one of the most common means of estimating the risks of radiation exposure resulting from population. The analysis of radionuclides in urban, agricultural and forest soils (e.g., Charro et al., 2013b) is important because of the bioresponsibility of soil as far as vegetation is concerned.

The major goal of this study is to identify the possible impact of radionuclide contamination resulting from former heavy industrial activities, namely from coal-fired power plants, in urban soils and attic dust in Salgótarján. For that purpose, the elemental content of U, Th, K and Cs and activity concentrations of three primordial radionuclides (^{226}Ra, ^{232}Th and ^{40}K) and one artificial radionuclide, which is a nuclear fission product (^{137}Cs), were determined in attic dust and urban soil samples. Since this study is the first to determine the presence of natural radionuclides in attic dust, it may provide new information about any potential risks of and the pathway for radionuclide contamination through urban areas.

2. Materials and methods

2.1. Study area

Salgótarján was a major mining and industrial city, which played a significant economic role in Hungary in the 19th and 20th centuries. The population today is approximately 35,000. The city is located in the northeastern part of Hungary encircled by the Karancs and Medves Hills at 220–500 m above sea level covering a total area of 103 km^2 (Fig. 1) in temperate continental climatic zone with variable weather conditions as well as distinguishable cold and warm seasons in addition to an average temperature of 8–9 °C (Bihari et al., 2018). The prevailing wind direction in the studied region is from the northwest with an average speed between 0.002 and 14.77 ms^{-1} (Tserendorj et al., 2022a). Rock formations covering the study area are volcanic (basalt and andesite) lavas and pyroclasts as well as sedimentary lithologies (mostly siliciclastic sandstone). Brown coal from the Miocene in Salgótarján embedded in sedimentary rock formations provided a local energy source. Brown forest soil is dominant in the wider region (Kercsmár et al., 2010).

Salgótarján was founded centuries ago and brown coal was discovered in the 1850's. Consequently, mining as well as the iron and steel industries commenced, moreover, the settlement began to grow rapidly, which was also promoted by the construction of a railway line between Salgótarján and Budapest (Wirth et al., 2012). During the following decades, approximately 17 million metric tons of brown coal was mined supporting a significant amount of investment in the iron and steel industries, associated companies and the local CFPP (Wirth et al., 2012). The city and its vicinity have been polluted as a consequence of coal mining, by-products of the CFPP, iron and steel works, the manufacture of mining machinery, glassworks, etc. Following this multi-industrial activity, the residues of coal combustion, like coal ash, as well as of steel and glass works, e.g., smelter and glass slag, were released into the environment without regulation and accumulated in the city, i.e., at the 'Pintértelep' coal ash cone (Fig. S1. A), 'Kucsord' slag hill and 'Inászó' brown coal tailing (Fig. 1). In 1973, the CFPP was decommissioned since local mining ceased due to the depletion of coal and its economic unviability. After the political regime change in 1990, economic activity decreased and heavy industry ceased, except for at the kitchen-stove factory (Fig. 1). However, a huge amount of waste remained throughout the city.

2.2. Sampling

Grid cells (1 × 1 km^2) covering the residential areas of Salgótarján were sampled. From each grid cell, one sample of attic dust was collected (Fig. 1; Table 1) by following the Euro-Geo-Surveys international urban geochemical sampling protocol (Demetriades and Birke,

2015). For this study, representative samples of urban soil were selected no further than 500 m from the corresponding sampling sites of attic dust. One sample of coal ash (CA) was collected from coal ash cone (Pintértelep; Fig. S1. A) and brown forest soil (BFS) from the forest to the northwest of the city (Fig. 1; Table 1) in August 2016.

2.2.1. Urban soil

A 'zig-zag' sampling technique (Alloway, 2013) was used where randomly chosen urban soil sampling points were selected based on the location of the desired 19 sampling sites, namely at the kindergarten (n = 3), playground (n = 7), park (n = 4) and others (n = 5; i.e., at the roadside, cemeteries and gardens) (Fig. 1; Table 1).

At each sampling point, 1–1.5 kg of disturbed soil was gathered from the organic-rich urban-soil horizon at a depth of 0–15 cm using a steel spade and steel hand auger before being mixed thoroughly to obtain a bulk sample. Since all our selected sampling points (Fig. 1; Table 1) are related to urban activities, the urban soil samples were considered to be disturbed (Richard et al., 2019). During the sampling, zip-lock polyethylene plastic bags (an effective means of transporting and storing dust as well as preventing cross-contamination) and powder-free nitrile skin-tight protective gloves made detailed work easier, waterproof and chemically resistant. All relevant information, such as photographs, GPS coordinates, land cover and soil types, the characteristics of the surroundings, the local history of development, the landscape and land use was recorded (Table 1).

2.2.2. Attic dust

Our attic dust sampling guidance protocol was primarily followed by Völgyesi et al. (2014a), b, in which papers other experiences (Cizdziel et al., 1998, 1999; Cizdziel and Hodge, 2000; Davis and Gulson, 2005; Gosar et al., 2006) were compiled.

The samples of attic dust from 36 buildings were collected from family houses (n = 27), churches (n = 4), kindergartens (n = 3) and blockhouses (n = 2) (Fig. 1; Table 1). Samples were taken from buildings built over 30 years ago where only a minimal amount of renovation had been carried out in their roofspace. The location and characteristics of each sampling site, that is, its type, year of construction, roof type, sampling surface and building materials, as well as other potential factors like its proximity to the CFPP were documented (Table 1). Dust away from the entrance to the attic and at the highest possible point of the ceiling was collected to minimize any possible disturbance as a result of residential activities as well as meet the expectations of undisturbed samples. The attic floor was not sampled, neither was organic material nor the remains of insects (Völgyesi et al., 2014a). Between 2 and 20 g of attic dust composed of 3–5 subsamples depending on the conditions were collected in polyethylene plastic bags using disposable fine brushes and nitrile protective gloves.

2.3. Sample processing for analysis

The samples of attic dust and urban soil were stored at room temperature until being processed for further analysis. According to Alakangas (2015), the 'coning and quartering' homogenization method was applied to ensure that a given amount of each sample is representive of its entirety. For the purpose of elemental analysis, all the samples of attic dust and urban soil, including brown forest soil and coal ash, were dried at 60 °C and sieved through a 0.180 mm mesh sieve. Additionally, the samples were pulverized by mild steel. The sample of coal ash was crushed, 70% of which was sieved through a 2 mm mesh sieve before being pulverized and 85% of this fraction sieved through a 0.075 mm mesh sieve. All pulverization and crushing techniques for the samples of urban soil, brown forest soil and coal ash were conducted at the Bureau Veritas Minerals Laboratories in Vancouver, Canada.

Regarding gamma spectrometric analysis, the samples of attic dust were sieved through a <0.125 mm mesh sieve to remove any agglomerated organic material (Cizdziel and Hodge, 2000; Ilacqua et al., 2003; Völgyesi et al., 2014a). The samples of urban soil, including brown forest soil and coal ash, were sieved through a <2.0 mm mesh sieve in line with studies undertaken on similar soils in Spain and Serbia (Charro et al., 2013a; Tanić et al., 2016). The samples were prepared in the Lithosphere Fluid Research Lab at Eötvös Loránd University in Budapest, Hungary.

2.3.1. ICP-MS elemental analysis

The content of U, Th and Cs (mg kg^{-1}) as well as K (m/m %) were determined in 57 urban geochemical samples, namely 36 of attic dust,

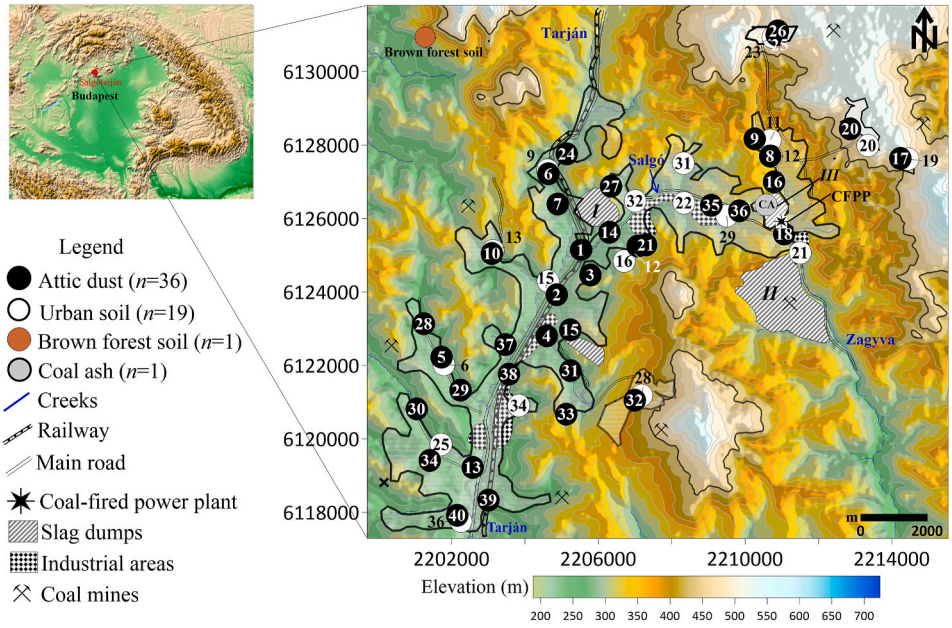

Fig. 1. The study area in Salgótarján, including sampling sites (attic dust, urban soil, brown forest soil and coal ash (CA)), location of the coal-fired power plant (CFPP) and slag dumps I, II and III (I - Kucsord Hill; II - former brown coal mine in Inászó; III - coal ash cone in Pintértelep). The residential area is marked by a contoured irregularly banded striped line. A topographic shaded relief image with contour lines denoting the elevation is overlaid. Local creeks (Tarján, Salgó and Zagyva) are indicated in blue. (For interpretation of the references to color in this figure legend, the reader is referred to the Web version of this article.)

Table 1
The elemental and activity concentrations of attic dust (n = 36), urban soil (n = 19), brown forest soil (n = 1) and coal ash (n = 1) samples as well as the categories of the sampling sites and their locations (x, y), elevation (m), types of housing and distance (km) from the coal-fired power plant (CFPP). Note that the locations of attic dust (x, y), elevation (m), types of housing and ^{137}Cs activity concentrations have already been published by Tserendorj et al. (2022a).

	Location			Activity concentration (Bq kg^{-1})				Elemental concentration of U, Th, Cs (mg kg^{-1}) and K (m/m %)					Category of sampling sites	Characteristics			Distance from CFPP
	X	Y	Elevation, m[1]	^{226}Ra	^{232}Th	^{40}K	^{137}Cs	U	Th	Th/U	K	Cs		Year of construction	Roof type	Sampling surface	m (*1000)
Attic dust (n = 36)																	
STN01AD	2205477	6124930	310	36.7 ± 3.5	29.4 ± 6.4	437.3 ± 28.6	15.9 ± 1.1	2.1	2.2	1.05	0.4	1.0	Church	1936	Metal	Concrete beam	3.7
STN02AD	2204815	6123910	324	39.8 ± 3.3	31.2 ± 6.0	442.5 ± 29.4	13.0 ± 1.3	2.1	4.5	2.14	0.3	1.4	Church	1914	Tile	Fiberglass envelope	4.4
STN03AD	2205749	6124438	309	35.8 ± 6.9	23.5 ± 6.6	658.7 ± 55.0	91.7 ± 6.0	3.4	3.0	0.88	1.0	2.0	Family house	1957	Tile	Wooden beam	3.7
STN04AD	2204534	6122799	270	23.3 ± 2.7	24.6 ± 5.3	309.2 ± 21.7	57.8 ± 3.1	1.4	3.1	2.21	0.2	1.4	Kindergarten	1980	Slate and tile	Concrete and wooden beam	4.8
STN05AD	2201621	6122238	254	42.9 ± 4.2	37.4 ± 6.9	518.5 ± 34.1	49.6 ± 3.1	2.9	3.7	1.28	0.6	2.1	Kindergarten	1990	Tile	Wooden beam	4.3
STN06AD	2204602	6127185	267	44.0 ± 5.4	29.1 ± 8.7	529.3 ± 40.9	162.3 ± 8.8	2.9	2.7	0.93	0.6	2.5	Family house	1960	Tile	Wooden beam	4.5
STN07AD	2204855	6126365	273	33.7 ± 5.2	27.8 ± 7.1	511.4 ± 42.4	104.1 ± 6.2	2.0	2.5	1.25	0.4	1.6	Family house	1944	Tile	Wooden beam	4.3
STN08AD	2210734	6127634	351	71.0 ± 5.4	49.9 ± 8.1	546.5 ± 35.9	126.5 ± 7.1	3.5	5.6	1.60	0.5	2.2	Kindergarten	1960	Slate	Wooden beam	1.3
STN09AD	2210308	6128102	349	20.5 ± 4.7	25.4 ± 12.1	513.9 ± 41.6	101.5 ± 5.6	2.5	3.4	1.36	0.5	1.6	Family house	1961	Slate	Wooden beam	1.8
STN10AD	2203028	6125036	287	22.0 ± 2.6	15.5 ± 5.8	422.2 ± 27.3	5.5 ± 0.9	1.0	2.1	2.10	0.2	1.1	Family house	1980	Slate	Wooden beam	5.4
STN12AD	2207059	6125216	307	16.4 ± 4.0	24.7 ± 9.5	486.2 ± 37.3	35.4 ± 2.5	1.9	2.9	1.53	0.8	1.3	Family house	1890	Slate	Wooden beam	2.7
STN13AD	2202467	6119246	233	34.9 ± 3.5	32.0 ± 6.8	487.5 ± 33.5	54.8 ± 3.4	1.8	3.8	2.11	0.3	1.0	Family house	1965	Slate	Wooden beam	7.2
STN14AD	2206280	6125594	275	16.7 ± 4.1	19.6 ± 9.0	501.5 ± 38.8	115.8 ± 6.7	2.0	3.3	1.65	0.7	1.5	Blockhouse	1950	Slate	Wooden beam	3.3
STN15AD	2205184	6122957	308	<dl	8.0 ± 2.6	368.1 ± 34.1	36.7 ± 2.7	4.1	1.3	0.32	0.7	2.1	Blockhouse	1965*	Tile	Wooden beam and metal timber	4.4
STN16AD	2210836	6126935	337	21.3 ± 2.8	21.7 ± 6.5	391.3 ± 26.6	93.9 ± 5.3	2.5	3.6	1.44	0.6	2.1	Family house	1970	Slate	Wooden beam	0.9
STN17AD	2214330	6127551	495	91.6 ± 6.4	61.0 ± 9.6	621.7 ± 43.3	169.8 ± 8.8	2.7	5.0	1.85	0.4	1.8	Family house	1922	Tile	Wooden beam	2.4
STN18AD	2211109	6125522	314	145.6 ± 8.3	83.9 ± 8.0	708.2 ± 41.4	35.7 ± 2.2	4.8	8.8	1.83	0.6	3.3	Family house	1970	Slate	Wooden beam	0.1
STN20AD	2212946	6128359	507	50.3 ± 8.2	20.1 ± 5.5	427.7 ± 55.6	123.4 ± 7.6	1.5	1.8	1.20	0.4	1.5	Family house	1960	Slate and tile	Wooden beam	2.2
STN21AD	2207291	6125248	305	56.0 ± 4.3	47.1 ± 6.5	533.5 ± 34.5	41.8 ± 2.6	2.9	4.8	1.66	0.4	2.0	Family house	1916	Tile	Wooden beam	2.5
STN24AD	2205113	6127722	276	17.9 ± 3.3	21.8 ± 8.2	522.8 ± 37.7	100.5 ± 5.6	1.4	2.7	1.93	0.3	1.3	Family house	1970	Slate	Wooden beam	4.2
STN25AD	2210931	6130914	492	31.0 ± 4.5	37.1 ± 8.9	568.6 ± 41.2	159.6 ± 8.4	2.0	3.4	1.70	0.6	0.9	Church	1930	Metal	Wooden beam	3.4
STN26AD	2210963	6131022	496	21.8 ± 2.4	24.5 ± 5.0	395.6 ± 25.7	41.3 ± 2.2	1.6	3.8	2.38	0.5	0.9	Family house	1920	Metal	Wooden beam	3.6
STN27AD	2206333	6126840	331	18.1 ± 3.4	16.3 ± 5.3	537.6 ± 38.2	90.3 ± 5.2	2.4	1.8	0.75	1.2	1.8	Family house	1940	Tile	Wooden beam	3.3

(*continued on next page*)

Table 1 (*continued*)

	Location			Activity concentration (Bq kg^{-1})				Elemental concentration of U, Th, Cs (mg kg^{-1}) and K (m/m %)					Category of sampling sites	Characteristics			Distance from CFPP
	X	Y	Elevation, m[1]	^{226}Ra	^{232}Th	^{40}K	^{137}Cs	U	Th	Th/U	K	Cs		Year of construction	Roof type	Sampling surface	m (*1000)
STN28AD	2201138	6123143	275	12.0 ± 6.0	24.5 ± 7.6	524.6 ± 38.5	51.0 ± 3.3	2.2	3.3	1.50	0.5	1.3	Church	1934**	Slate	Wooden beam	6.9
STN29AD	2202141	6121341	245	15.7 ± 5.3	18.8 ± 7.4	417.6 ± 30.3	117.8 ± 6.6	1.7	3.0	1.76	0.4	1.4	Family house	1936	Tile	Wooden beam	6.6
STN30AD	2200930	6120839	253	38.7 ± 5.4	28.7 ± 9.2	477.4 ± 38.8	70.7 ± 4.5	2.1	3.0	1.43	0.5	1.4	Family house	1950	Slate	Wooden beam	7.5
STN31AD	2205184	6121852	267	85.5 ± 7.4	47.0 ± 13.1	607.7 ± 49.9	77.1 ± 5.1	2.2	4.1	1.86	0.4	1.5	Family house	1910	Slate and wood	Wooden beam	4.7
STN32AD	2206954	6121042	412	92.5 ± 7.8	42.8 ± 12.4	563.6 ± 45.8	165.8 ± 8.9	2.4	2.4	1.00	0.4	1.9	Family house	1900	Tile	Wooden beam	3.0
STN33AD	2205060	6120675	299	13.6 ± 3.8	21.2 ± 9.4	411.4 ± 35.2	137.8 ± 7.9	1.9	2.2	1.16	0.5	1.8	Family house	1955	Tile	Wooden beam	5.2
STN34AD	2201280	6119441	261	42.8 ± 6.5	30.3 ± 13.6	514.6 ± 48.9	169.3 ± 9.4	2.0	2.2	1.10	0.6	1.5	Family house	1936	Tile	Wooden beam	7.8
STN35AD	2209100	6126310	306	143.5 ± 8.1	94.3 ± 9.6	649.9 ± 43.2	41.6 ± 2.5	5.6	10.5	1.88	0.6	3.2	Family house	1946	Slate	Wooden beam	1.4
STN36AD	2209873	6126154	306	63.5 ± 5.9	63.1 ± 11.2	649.8 ± 47.8	87.3 ± 5.0	3.6	6.0	1.67	0.6	2.4	Family house	1940	Tile	Wooden beam	0.9
STN37AD	2203389	6122568	253	69.2 ± 5.2	44.1 ± 7.8	559.9 ± 38.2	124.7 ± 6.5	3.2	4.0	1.25	0.5	1.7	Family house	1961	Tile	Wooden beam	5.6
STN38AD	2203483	6121767	245	35.3 ± 3.5	39.0 ± 7.8	510.0 ± 36.0	73.9 ± 4.3	1.7	3.5	2.06	0.3	1.4	Family house	1880	Tile and wood	Wooden beam	5.7
STN39AD	2202896	6118359	237	32.6 ± 3.4	32.6 ± 6.7	530.0 ± 33.8	93.6 ± 5.0	1.5	2.6	1.73	0.4	1.2	Family house	1880***	Tile	Wooden beam	7.3
STN40AD	2202031	6117952	230	27.2 ± 4.0	27.7 ± 8.4	1382.3 ± 77.6	149.0 ± 7.7	2.2	1.7	0.77	2.7	1.4	Family house	1964****	Tile	Wooden beam	8.0
Year of renovation of house: *2006; ** 2013; ***1984; ****1991; dl: detection limit; 0.9 Bq kg^{-1} m 1 - house height is added to elevation, m.																	
Urban soil (n = 19)																	
STN06US	2201685	6122038	244	18.2 ± 1.2	21.7 ± 2.4	357.8 ± 8.0	4.7 ± 0.4	0.9	4.4	4.89	0.2	1.0	Kindergarten				6.5
STN09US	2204580	6127284	265	36.2 ± 1.5	48.8 ± 3.6	412.9 ± 8.8	6.3 ± 0.5	1.8	5.4	3.00	0.3	1.9	Park				4.4
STN11US	2210741	6128060	356	19.7 ± 1.3	28.0 ± 2.5	391.9 ± 8.1	6.5 ± 0.5	0.7	3.4	4.86	0.3	1.3	Park		.		1.7
STN12US	2210769	6127625	340	21.3 ± 1.4	26.5 ± 3.9	363.7 ± 9.0	7.4 ± 0.3	0.8	2.9	3.63	0.2	1.0	Kindergarten				1.5
STN13US	2203061	6125110	281	27.2 ± 1.3	42.8 ± 3.0	447.7 ± 8.4	3.1 ± 0.4	0.8	6.2	7.75	0.4	1.7	Kindergarten				5.4
STN15US	2204580	6124278	245	15.0 ± 1.3	25.0 ± 3.5	403.0 ± 8.4	2.7 ± 0.5	0.9	3.6	4.00	0.2	1.2	Playground				4.4
STN16US	2206684	6124811	297	33.2 ± 1.9	35.6 ± 6.0	347.5 ± 10.6	2.7 ± 0.7	1.2	4.5	3.75	0.3	1.3	Playground				2.9
STN19US	2214540	6127535	492	24.8 ± 1.4	38.8 ± 2.9	404.3 ± 8.7	13.6 ± 0.6	1.8	3.9	2.17	0.3	1.1	Park				2.8
STN20US	2213437	6127905	540	30.4 ± 1.6	40.5 ± 5.0	428.5 ± 10.7	17.3 ± 0.4	1.2	3.3	2.75	0.2	1.0	Playground				2.2
STN21US	2211549	6125012	377	33.7 ± 1.4	34.0 ± 3.9	344.8 ± 9.2	7.8 ± 0.3	1.5	3.7	2.47	0.3	1.2	Others (roadside)				0.5
STN22US	2208343	6126379	394	24.5 ± 2.8	26.9 ± 0.7	355.7 ± 7.2	1.1 ± 0.2	0.8	4.6	5.75	0.3	1.2	Others (roadside)				1.8

(*continued on next page*)

Table 1 (*continued*)

	Location			Activity concentration (Bq kg^{-1})				Elemental concentration of U, Th, Cs (mg kg^{-1}) and K (m/m %)					Category of sampling sites	Characteristics			Distance from CFPP
	X	Y	Elevation, m[1]	^{226}Ra	^{232}Th	^{40}K	^{137}Cs	U	Th	Th/U	K	Cs		Year of construction	Roof type	Sampling surface	m (*1000)
STN23US	2210832	6130849	482	17.7 ± 1.2	18.9 ± 2.3	373.2 ± 7.5	4.6 ± 0.4	1.2	4.3	3.58	0.2	1.1	Playground				3.6
STN25US	2201596	6119873	232	17.0 ± 1.0	26.3 ± 2.1	391.4 ± 7.0	2.3 ± 0.4	1.1	4.3	3.91	0.3	1.1	Playground				7.2
STN28US	2207146	6121173	400	21.1 ± 1.2	34.9 ± 2.3	397.6 ± 7.3	12.8 ± 0.5	1.0	2.8	2.80	0.3	0.9	Playground				3.8
STN29US	2209527	6126021	293	38.3 ± 1.4	46.0 ± 2.6	385.4 ± 7.7	4.3 ± 0.5	2.3	5.8	2.52	0.4	1.8	Playground				1.1
STN31US	2208334	6127451	331	26.4 ± 3.3	22.3 ± 0.6	355.5 ± 10.3	0.7 ± 0.2	0.8	3.2	4.00	0.3	1.0	Others (garden)				2.2
STN32US	2206997	6126439	274	27.2 ± 2.0	37.0 ± 7.4	398.6 ± 11.9	1.6 ± 0.8	1.3	5.4	4.15	0.3	1.2	Park				2.7
STN34US	2203747	6120914	245	21.3 ± 1.4	28.1 ± 3.7	409.8 ± 9.0	3.5 ± 0.5	1.0	4.6	4.60	0.3	1.1	Others (roadside)				5.6
STN36US	2202135	6117791	231	23.9 ± 1.1	41.4 ± 2.4	371.8 ± 6.9	3.5 ± 0.4	0.6	6.5	10.83	0.2	1.2	Others (cemetery)				7.8
Brown forest soil (BFS)	2200292	6131104	249	14.1 ± 1.3	15.7 ± 2.3	318.8 ± 9.0	18.4 ± 0.6	1.0	3.0	3.00	0.2	2.1	Undisturbed soil				8.1
Coal ash (CA)	2210737	6125749	351	91.1 ± 1.7	69.5 ± 3.3	414.4 ± 8.9	0.09 ± 0.4	6.3	12.8	2.03	0.5	2.7	Production of CFPP				0.5

CFPP - Coal-fired power plant.

19 of urban soils, 1 of brown forest soil (BFS) and 1 of coal ash (CA) (Fig. 1; Table 1). For this purpose, single quadrupole inductively coupled plasma mass spectrometry (ICP-MS) was applied. Each sample was dried and pulverized by following the aforementioned preparation methods. After each homogenization, ~1 g of attic dust or 15 g of urban soil samples were digested in modified aqua regia (1:1:1 - HNO_3: HCl: H_2O) at 95 °C for 1 h until the soil solution had been completely digested (Reimann et al., 2009) in the Bureau Veritas Minerals Laboratories in Vancouver, Canada. The analytical quality was controlled using certified reference material STD DS11 for U, Th and Cs (mg kg^{-1}) and K (m/m %). The analyzed (average) and expected elemental content for STD DS11 are 2.70 and 2.59 mg kg^{-1} for U (% recovery: 104.2), 7.60 and 7.65 mg kg^{-1} for Th (% recovery: 99.3), 2.72 and 2.88 mg kg^{-1} for Cs (% recovery: 94.4) as well as 0.40 and 0.40 m/m % for K (% recovery: 100), respectively.

2.3.2. Gamma spectrometric analysis

For urban soils, on average 100–150 g of the homogenized samples (urban soil, brown forest soil and coal ash) was placed in a special theoretically radon-leakage-free sample container made of HDPE because this material has advantageous mechanical and radon-permeability characteristics (Kis et al., 2013). Measurements were taken in a DÖME[1] low-background counting chamber at the Nuclear Analysis and Radiography Department at the Centre for Energy Research, Hungary. The n-type HPGe detector (Type: Canberra GR1319) had a relative efficiency of 13%, whereas the energy resolution (FWHM) was 1.53 and 1.99 keV at 662 and 1332 keV, respectively.

The samples of attic dust were placed in closed cylindrical polyethylene plastic vials, while keeping the sample height constant at 1.7 mm and varying the mass (mean 1.77 ± 0.48 g). The prepared samples were placed in a well-type HPGe detector with a hole of 14 mm in diameter and 40 mm in depth. The active volume of the detector is 300 cm^3. A Canberra GCW 6023 well-type HPGe detector was used with a relative efficiency of 62.8%, a full width at half maximum (FWHM) of 1.39 keV at 122 keV (^{57}Co) and 2.13 keV at 1332 keV (^{60}Co) as well as a peak/Compton ratio of 63.3/1. The detector was placed in a low-background counting chamber with a 30 cm thick pre-WWII iron shield composed of Cu to reduce interference from natural background radiation. Measurements were carried out at the Nuclear Security Department at the Centre for Energy Research, Hungary. To determine the concentrations of natural long-lived radionuclides in a low activity of samples, e.g., sediment cores and atmospheric aerosols, a well-type HPGe detector was developed by Barba-Lobo et al. (2021). In γ-spectrometric measurements, large amounts of material are usually used (approximately up to 1000 g). However, a well-type HPGe detector is ideal for small amounts of environmental samples as it combines a low background radiation limit with a high detection efficiency due to the 4π solid angle as well as shorter counting times (Canberra, 2000; Laborie et al., 2000), which was used in the present study.

All the samples were placed in the holder at least one month before measurements were taken to reach secular equilibrium between ^{226}Ra and its progenies. Gamma spectrometric measurements were performed over live times varying between 86,400 and 604,800 s. Analyses were carried out using FitzPeaks (Version 3.71) software. The activity concentrations were determined for the following set of radionuclides (the selected gamma lines appear in brackets): ^{137}Cs (661.9 keV), ^{40}K (1460.8 keV), ^{232}Th (238.6 keV of ^{212}Pb; 583 keV of ^{208}Tl; 727 keV of ^{212}Bi and 911 keV of ^{228}Ac) and ^{226}Ra (295.2 and 351.9 keV of ^{214}Pb) as well as the decay series of ^{238}U. To determine the distribution of background radiation in the environment around the detector, an empty container of the same geometry was counted using the same method as the samples. The background spectra were used to correct the net peak area of γ-rays produced by the measured isotopes. The level of precision,

[1] The Hungarian acronym of "Extremely Heavy Measurement Instrument'.

obtained by analysing field duplicates, differed by less than 10% as measured by the ratio of the average RMSE (root mean square error). All the results regarding the reduction in the ^{137}Cs activity concentrations were corrected according to the sampling date of August 2016 (sampling time).

The quality control sample, which was measured and evaluated along with the real samples, was made of moss-soil (reference material IAEA-447). The activity concentrations of this radionuclide found in the samples of attic dust and urban soil were considered in a standard procedure, i.e. using the total net counts under the photopeak, the measured photopeak efficiency, gamma-ray intensity and mass of the sample in grams. The minimum detectable activity of each radionuclide was obtained following the method applied by Currie (2004).

2.4. Statistical analysis

To obtain an overview of the data, descriptive statistics were calculated and presented on box and whisker plots (e.g., Kovács et al., 2012). The outlying values were determined according to the inner-fence criteria (Tukey, 1977).

For an in-depth analysis and comparison of the attic dust and urban soil samples, first the data was tested for normal distribution using the Shapiro-Wilk test (Shapiro and Wilk, 1965) since the sample size was rather low ($n < 50$) (Ghasemi and Zahediasl, 2012; Reimann et al., 2008) (Table 2). To test the similarity between the median activity concentrations (^{226}Ra, ^{232}Th, ^{40}K and ^{137}Cs in Bq kg^{-1}) of the measured radionuclides in the samples of attic dust and urban soil, the Wilcoxon Mann-Whitney homogeneity test (Mann and Whitney, 1947) was used. The linear relationship between radionuclides, regardless of their origin, was explored using the non-parametric Spearman's correlation (Schober and Schwarte, 2018). The effect of predictors, namely the distance from (km) and elevation above (m) the coal-fired power plant, as well as of the measured radionuclide activities was assessed using bivariate least squares regression analysis (Reimann et al., 2008) with the relationship regarded as significant at $p < 0.05$.

To obtain a representative interpolated map of the measured radionuclide activities, geostatistical analysis was conducted (Webster and Oliver, 2007). For each radionuclide, variogram was used as a tool to describe the spatial autocorrelation structure of the radionuclides and obtain the weights necessary to predict their values in surrounding unsampled areas using kriging (e.g., Hatvani et al., 2017). Specifically, empirical semivariograms were calculated on which theoretical ones were fitted using least squares fitting and the Matheron algorithm (Matheron and Marie, 1965). Next, ordinary point kriging was used to obtain the interpolated maps (Cressie, 1990). Inverse distance weighting (Lu and Wong, 2008) was performed to obtain an interpolated map of ^{40}K. All the ranges of coordinates reported in the study area are planar distances in km (EPSG: 3857). All computations were done in IBM SPSS 25.0, STATIGRAPH, whereas geostatistical mapping was carried out using Golden Software 15.3 and GS +10.

2.5. Radiological assessment

Possible health effects, due to external exposure to natural gamma radiation, were estimated based on the obtained results for the radionuclide activities of ^{226}Ra, ^{232}Th, ^{40}K and ^{137}Cs (Bq kg^{-1}) in the samples of urban soil since the upper layer of urban soil is considered to contribute towards the external gamma radiation. To assess the risk the population residing near to the CFPP and slag dumps are exposed to (Fig. 1), the total absorbed gamma dose rate (D) (nGy h^{-1}) [Eq. (1)] and annual effective dose (E) (mSv y^{-1}) were calculated for the samples of urban soil. Although the total absorbed gamma dose rate (D) calculation is for extended materials, e.g., building materials, as an estimation, it was calculated for the samples of attic dust and coal ash too.

The total absorbed gamma dose rate (D) (nGy h^{-1}) in the air 1 m above ground level was estimated using Eq. (1) provided by the UNSCEAR 2008 Report (UNSCEAR, 2010). The equation was modified to include the contributions of the artificial radionuclide ^{137}Cs. The given dose coefficient of ^{137}Cs is 0.124 nGy h^{-1} according to Antovic et al. (2012). These factors are representative of the absorbed dose rates in air per unit activity per unit of sample mass.

$$D\ (\mathrm{nGy\ h^{-1}}) = 0.462(^{226}\mathrm{Ra}) + 0.604(^{232}\mathrm{Th}) + 0.0417(^{40}\mathrm{K}) + 0.124(^{137}\mathrm{Cs}) \quad [1]$$

The annual effective dose (E) (mSv y^{-1}) was calculated using a conversion factor of 0.7 (Sv Gy^{-1}) to convert the absorbed dose in air (D) (nGy h^{-1}) into the effective dose rate of environmental gamma radiation that adults are exposed to by taking into account the outdoor occupancy factor (fraction of time spent outdoors) of 0.2, that is, 8760 h y^{-1}, proposed by the UNSCEAR, 2010. Accordingly, the annual effective dose (E) was calculated by Eq. (2):

$$E\ (\mathrm{mSv\ y^{-1}}) = D\ (\mathrm{nGy\ h^{-1}}) * 8760\ (\mathrm{h\ y^{-1}}) * 0.2 * 0.7\ (\mathrm{Sv\ Gy^{-1}}) * 10^{-6} \quad [2]$$

3. Results and discussion

3.1. Elemental concentration of U, Th, K and Cs in urban soil and attic dust

In urban soil, content ranges of U (mg kg^{-1}), Th (mg kg^{-1}) and K (m/m %) varied from 0.6 to 2.3 (mean: 1.1), 2.8 to 6.5 (mean: 4.4) and 0.2 to 0.4 (mean: 0.3), respectively, which are higher than those of brown forest soil, namely 1.0 to 3.0 and 0.2, respectively (Fig. 2A–C; Table S1). However, in the attic dust, the content of U (1.0–5.6; mean: 2.4 mg kg^{-1}), K (0.2–2.7; mean: 0.6 m/m %) and Cs (0.9–3.3; mean: 1.7 mg kg^{-1}) were higher than in the samples of urban soil and brown forest soil (Fig. 2A, C and D; Table S1). In contrast, lower mean value was obtained

Table 2
Summary statistics of the activity concentrations (Bq kg^{-1}) of ^{226}Ra, ^{232}Th, ^{40}K and ^{137}Cs in samples of attic dust (n = 36) and urban soils (n = 19) from Salgótarján.

		Mean	Median	St.dev.	Min.	Max.	Mann-Whitney (Wilcoxon) test[a]	Shapiro – Wilk normality test[b]
^{226}Ra	Attic dust	43.3 ± 4.6	35.1	33.8	12.0 ± 6.0[c]	145.6 ± 4.3	**0.03**	0.00
	Urban soil	25.2 ± 1.6	24.5	6.8	15.0 ± 1.3	38.3 ± 1.4		**0.47***
^{232}Th	Attic dust	34.0 ± 18.7	28.9	18.2	8.0 ± 9.0	94.3 ± 9.6	0.52	0.00
	Urban soil	33.0 ± 3.2	34	8.7	18.9 ± 2.3	48.8 ± 3.6		**0.53***
^{40}K	Attic dust	534.4 ± 39.1	516.6	169.6	309.2 ± 21.7	1382.3 ± 76.6	**0.00**	0.00
	Urban soil	386.4 ± 8.6	391.5	28.4	344.8 ± 9.2	447.8 ± 8.4		**0.98***
^{137}Cs	Attic dust	88.5 ± 5.1	91	47.9	5.5 ± 0.9	169.8 ± 2.9	**0.00**	**0.18***
	Urban soil	6.0 ± 0.4	4.3	4.5	0.7 ± 0.2	17.3 ± 0.4		0.00

[a] Reject the null hypothesis for alpha >0.05, bolded values show that the medians area significantly different.
[b] p significance values are greater than >0.05, bolded data are normally distributed* Shapiro-Wilk normality tests.
Brown forest soil (BFS) and coal ash (CA) are not included in this table.
[c]Note that among the^{226}Ra activity concentrations there was one sample below the detection limit (Bq kg^{-1}).
[c] Note that among the^{226}Ra activity concentrations there was one sample below the detection limit (Bq kg^{-1}).

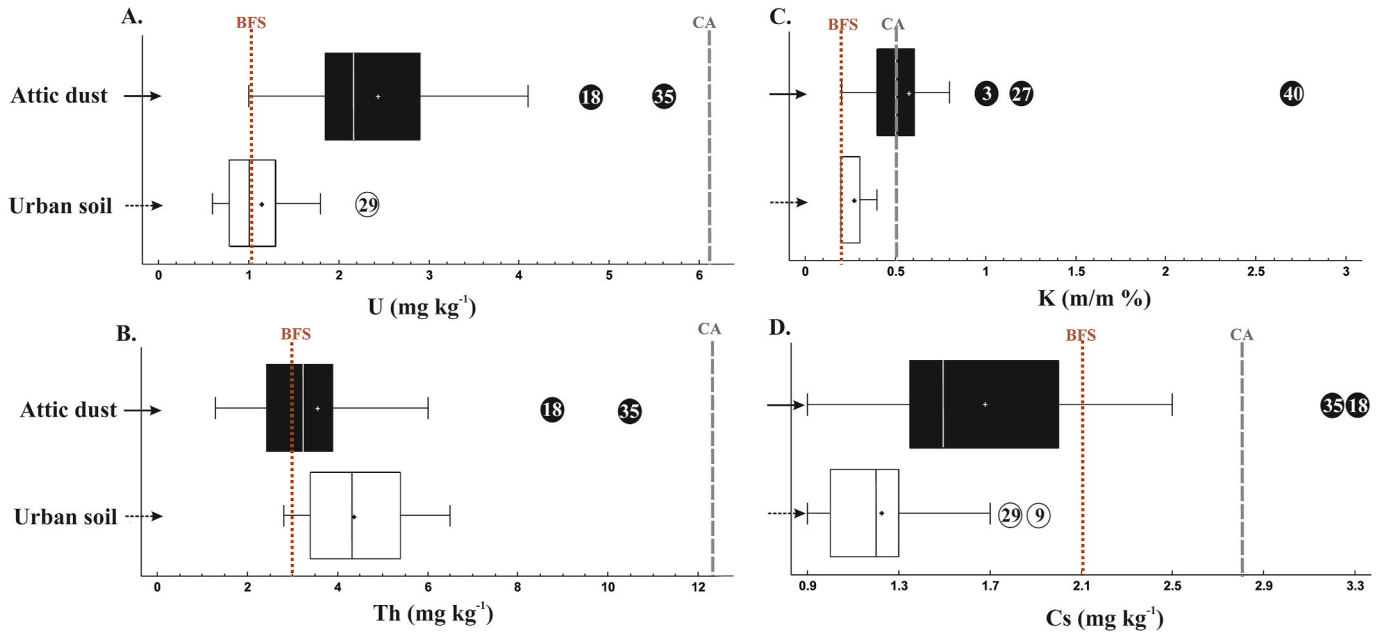

Fig. 2. Box and whisker plot of the elemental concentration of U, Th and Cs in mg kg^{-1} and of K in m/m % in 36 attic dust and 19 urban soil samples from Salgótarján. Brown forest soil (BFS) and coal ash (CA) samples are denoted by vertical brown and grey lines, respectively. (For interpretation of the references to color in this figure legend, the reader is referred to the Web version of this article.)

for Th in attic dust (3.6 mg kg^{-1}) than that in urban soil (4.4 mg kg^{-1}), except for two outlying attic dust samples, that is, STN18AD – family house: 8.8 and STN35AD – family house: 10.5 mg kg^{-1} (Fig. 2B; Tables 1 and S1). The content of U, Th and Cs in coal ash (6.3, 12.8 and 2.7 mg kg^{-1}, respectively) are higher than those in the samples of attic dust, urban soil and brown forest soil (Fig. 2 A, B and D; Table 1). However, the K content in coal ash is lower (0.5 m/m %) than the mean value in attic dust and higher than that in urban soil (Fig. 2C; Table 1).

The U-Th-K triplot graphically depicts the ratios of these three elements in different media (Fig. 3). Variations in the U-Th-K triplot in the studied samples show a close relationship between the U and Th content, creating a closed cluster along the U-Th axis with that of U gradually

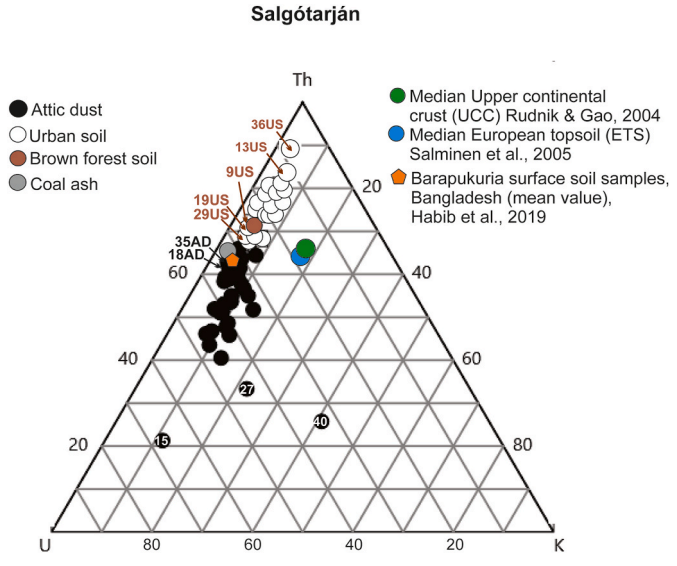

Fig. 3. Variation in U-Th-K content in Salgótarján urban soil (white circle), attic dust (black circle), brown forest soil (brown circle) and coal ash (grey circle) samples. Values of U and Th (mg kg^{-1}) as well as K (m/m %) were normalized to 100. (For interpretation of the references to color in this figure legend, the reader is referred to the Web version of this article.)

increasing when comparing the Th content of attic dust samples with urban soil ones (Fig. 3). Local samples of coal ash and brown forest soil also fell into this cluster (Fig. 3). The former fell within the field of attic dust samples in the vicinity of the two outlying attic dust samples, namely STN18AD – family house and STN35AD – family house (Figs. 1 and 2A; Table 1), close to the three outlying U urban soil ones, that is, STN29US – playground, STN19US – park and STN09US – park (Figs. 1, 2A, 3; Table 1). Although the brown forest soil fell within the range of the urban soil samples (Fig. 3; Table 1), the two samples of urban soil containing the highest Th content, namely STN13US – kindergarten: 6.2 mg kg^{-1} and STN36US – others (cemetery): 6.5 mg kg^{-1} (Figs. 1, 2B, 3; Table 1), exhibit the lowest U content, revealing the geochemical nature of U during chemical weathering in an oxidative environment. Under these circumstances, U^{6+} is highly soluble and can be leached out from the urban soil (Salminen et al., 2005). In contrast, Th (in the form of Th^{4+}) remains immobile (Salminen et al., 2005) in resistant minerals like zircon in urban soil or is adsorbed onto the surface of clay minerals and organic substances (Cinelli et al., 2019). This alteration mechanism is an important factor in terms of the U-Th distribution in urban soils in Salgótarján causing a general U loss, except for in sample STN29US - playground (Figs. 1, 2A, 3; Table 1). Uranium enrichment in this urban soil sample probably derived from the continuous supply of U-Th over several decades from the local coal ash cone, since this sampling site is 1100 m away from the coal ash cone (Fig. 1; S1-A), which is a clear indication of the local pollution source. Additionally, the distribution of the upper continental crust (UCC) and European topsoil (ETS) values (Rudnick and Gao, 2004; Salminen et al., 2005) along with three outlying samples of attic dust, namely STN15AD – blockhouse, STN27AD – family house and STN40AD – family house (Fig. 3), are distinguishable due to their particular compositions. The K_2O content of attic dust sample STN40AD – family house is significantly elevated, even compared to UCC and ETS (Fig. 3; Table S1). The residents in this house stored K-fertilizer in their attic or other unknown anthropogenic sources which could increase K levels. The outlier, that is, STN27AD – family house, exhibits the second lowest Th/U ratio (0.75; Table 1) in the studied area. Similarly, a low Th/U ratio is characteristic of the attic dust in the samples of STN03AD – family house and STN06AD – family house collected in the vicinity of one of the slag dumps called Kucsord Hill

(Fig. 1). Moreover, attic dust from STN15AD – blockhouse shows the lowest Th/U ratio (0.32) and an elevated U content (4.1 mg kg^{-1}), strongly distorting the observed relationship between U and Th in this sample (Fig. 3, S2-A; Table 1). This unusual sample of attic dust derived from a two-storey attic whose roof was renovated, i.e., the roof tiles were changed, in 2006 (Table 1). Therefore, the accumulation time of the attic dust was only approximately 12 years since the environment changed, during which time the majority of the industrial factories had already been shut down. Consequently, this sampling site provided one of the smallest amounts of attic dust collected in Salgótarján (~3 g) with a highly elevated U content derived from an unknown source. It should be noted, however, that structure composed of metal timber was observed (Table 1) in the attic, which is an unusual occurrence in the study area (Figs. S2–C).

Studies on the chemical compositions of soils in the vicinity of a CFPP from Bangladesh have already been published (Habib et al., 2019), from where the authors reported 4-9 times higher U and 5-7 times higher Th content in their soil samples than in those from samples of urban soils and attic dust in Salgótarján, respectively (Fig. 3). Significant differences in the U and Th content between urban soils from Salgótarján and Bangladesh can be explained by the differences in the chemical composition between the coal ash present in both areas in the urban soils.

The highest concentrations of U (6.3 mg kg^{-1}) and Th (12.8 mg kg^{-1}) occur in the coal ash sample in Salgótarján (Fig. 2; Table 1), supporting that by-products from the CFPP are significant sources of U and Th enrichment in the studied samples, similarly to studies published from other countries e.g., Lauer et al. (2015); Llorens, 2001. However, it should be noted that only one coal ash sample was studied in Salgótarján, the U and Th concentrations of which are lower than those from Poland (Silesia: 20.7 and 13.6 mg kg^{-1} as well as Lublin: 17.2 and 18.2 mg kg^{-1}, respectively; Parzentny and Róg, 2019), Spain (22.9 and 22.1 mg kg^{-1}, respectively; Llorens, 2001), Turkey (34 and 22 mg kg^{-1}, respectively; Finkelman, 1993); China (<51.9 and < 50 mg kg^{-1}, respectively; Dai et al., 2014) and Bangladesh (26.6 and 65.1 mg kg^{-1}, respectively; Habib et al., 2019). These data on coal ash samples are indicative of significance differences in the local geology, including the age of mined coal and physical (particularly meteorological) conditions, as well as the operational technology of the power plant and repository methods of by-products discussed below.

3.2. Activity concentrations of the radionuclides ^{226}Ra, ^{232}Th, ^{40}K and ^{137}Cs

3.2.1. Urban soil

The activity concentrations of ^{226}Ra, ^{232}Th, ^{40}K and ^{137}Cs (in Bq kg^{-1}) in the samples of urban soil from Salgótarján vary from 15.0 ± 1.3 to 38.3 ± 1.4 (mean: 25.2 ± 1.6), 18.9 ± 2.3 to 48.8 ± 3.6 (mean: 32.8 ± 3.2), 344.8 ± 9.2 to 447.8 ± 8.4 (mean: 386.4 ± 8.6) and 0.7 ± 0.2 to 17.3 ± 0.4 (mean: 5.6 ± 0.4), respectively (Fig. 4; Tables 1-2). The only one outlier in the urban soil datasets is the ^{137}Cs value 17.3 ± 0.4 (STN20US - playground).

All of the studied urban soil samples exhibit higher ^{226}Ra, ^{232}Th and ^{40}K concentrations than the one of brown forest soil (BFS) (14.1 ± 1.3, 15.7 ± 2.3 and 318.8 ± 9.0, respectively), whereas all of them contain lower ^{137}Cs concentrations than the BFS sample (18.4 ± 0.6) (Figs. 1, 4A-D; Table 1). Hence the local brown forest soil is considered to be a significant natural geogenic contribution to the studied urban soil samples.

Three urban soil samples, namely STN29US from a playground, STN09US from a park and STN21US from others (roadside) (Fig. 1), exhibit the highest ^{226}Ra (38.3 ± 1.4, 36.2 ± 1.5 and 33.7 ± 1.4, respectively) and ^{232}Th (46.0 ± 2.6, 48.8 ± 3.6 and 34.0 ± 3.9 Bq kg^{-1}, respectively) concentrations among the urban soils (Fig. 5; Table 1). Urban soil STN09 - park (which also exhibits an elevated elemental Th concentration (Figs. 4–5; Tables 1-2) is close to one of the largest slag dumps in the city called Kucsord Hill (Fig. 1), moreover, STN21US – others (roadside) and STN29US - playground are of closest to the CFPP, suggesting the coal ash has a significant contribution to the studied urban soils discussed later.

The ^{226}Ra-^{232}Th-^{40}K triplot graphically depicts the ratios of these three radionuclides in different media (in the studied urban soil, brown forest soil, attic dust and coal ash) (Fig. 5). For the purpose of a comparison, the same activity concentration values of surface soils and attic dust in the vicinity of other CFPP are also indicated in the plot. (Note that coal ash and attic dust are compared later in Chapters 3.2.2 and

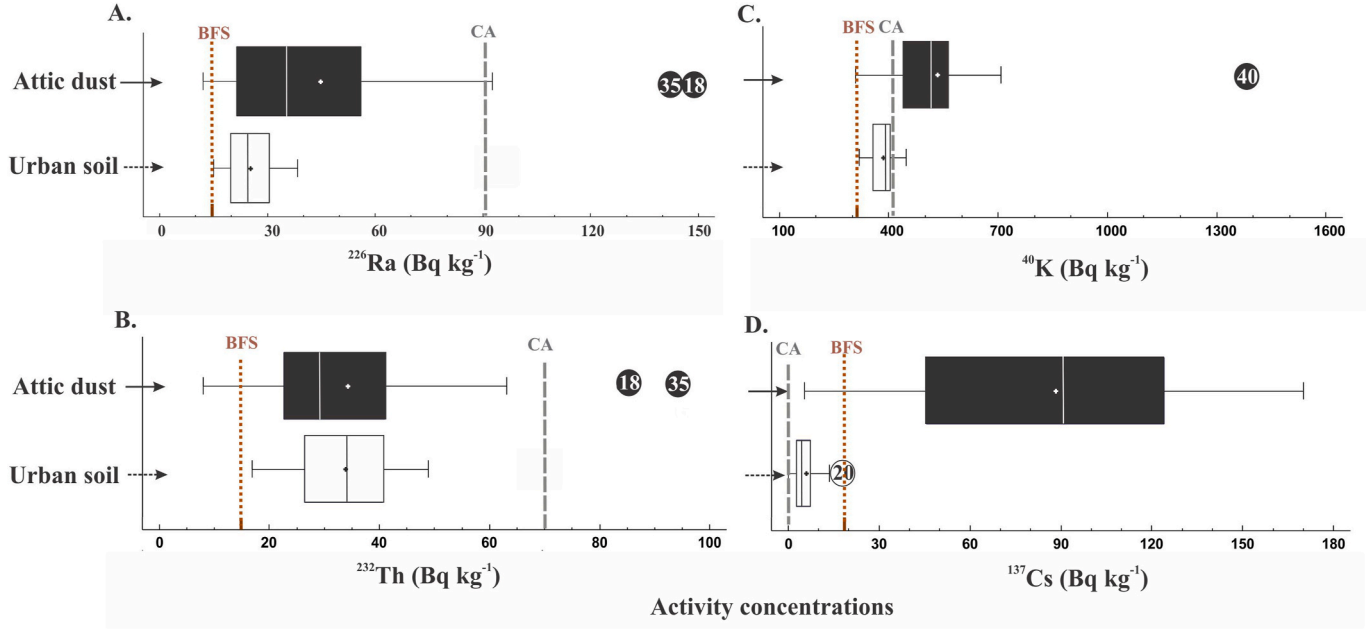

Fig. 4. Box and whisker plot of the activity concentrations of ^{226}Ra, ^{232}Th, ^{40}K and ^{137}Cs in 36 attic dust and 19 urban soil samples from Salgótarján. The brown forest soil (BFS) and coal ash (CA) samples are denoted by vertical brown and grey lines, respectively. (For interpretation of the references to color in this figure legend, the reader is referred to the Web version of this article.)

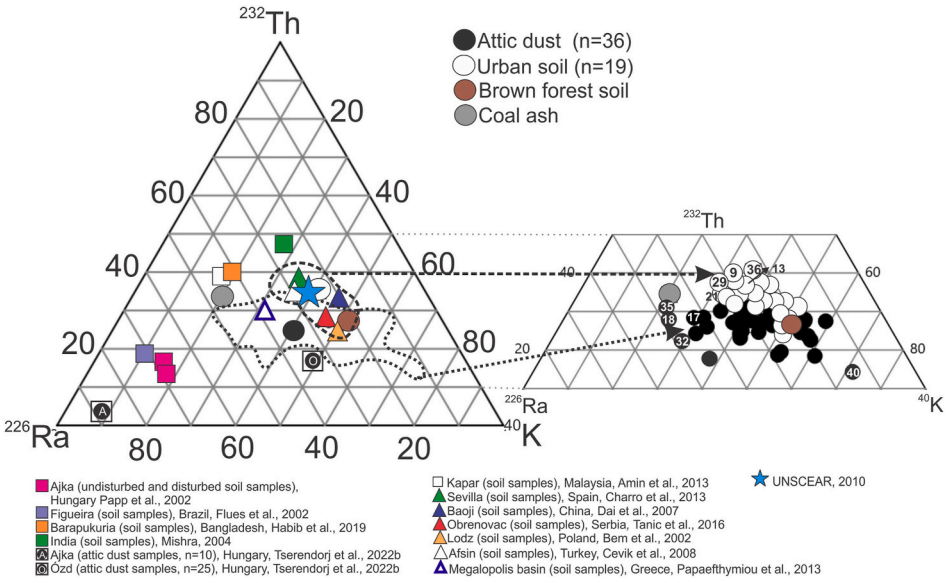

Fig. 5. Variation in the ^{226}Ra-^{232}Th-^{40}K activity concentrations in samples of urban soil (white circles), attic dust (black circles), brown forest soil (brown circle) and coal ash (grey circle) from Salgótarján. The dashed line shows the extent of the urban soil samples, whereas the dotted line shows the extent of the attic dust ones. The other colored symbols show the mean values for surface soils found in the literature. The activity concentrations were normalized to 100, but those of ^{40}K were divided by 10 to compare this radionuclide more easily. (For interpretation of the references to color in this figure legend, the reader is referred to the Web version of this article.)

3.2.3.) The activity concentrations of urban soils in Salgótarján fall within the mean values from China (Dai et al., 2007), Greece (Papaefthymiou et al., 2013), Poland (Bem et al., 2002), Serbia (Tanić et al., 2016), Spain (Charro et al., 2013a) and Turkey (Cevik et al., 2008) (Fig. 5; Table 3). Note that the brown forest soil and mean values of soils worldwide (not only in the vicinity of CFPP) also fall within those

Table 3
Comparison of the mean and range of activity concentrations (Bq kg^{-1}) of ^{226}Ra, ^{232}Th, ^{40}K and ^{137}Cs in samples of urban soils and attic dust from Salgótarján as well as of surface soils in the vicinity of coal-fired power plants worldwide. The medians of soil samples worldwide (not just in the vicinity of CFPPs) are also shown (UNSCEAR, 2000).

Locality	Type of the samples	Activity concentrations (Bq kg^{-1}), mean (min - max)				References
		^{226}Ra	^{232}Th	^{40}K	^{137}Cs	
Salgótarján city, Hungary	Attic dust n = 36 (undisturbed)	43 (12*[1]-145)	34 (8 - 94)	534 (309 - 1382)	88 (5 -169)	This study
Salgótarján city, Hungary	Urban soil n = 19 (disturbed, 0–15 cm)	25 (15 - 38)	33 (18 - 48)	386 (344 - 447)	6 (0.7 - 17)	This study
Ózd, Hungary	Attic dust n = 25 (undisturbed)	31 (2*[X] - 62)	16 (8 - 26)	400 (80 - 1493)	88 (2 - 272)	Tserendorj et al. (2022b)
Ajka, Hungary	Attic dust n = 10 (undisturbed)	318 (64 - 587)	21 (15 - 31)	442 (190 - 1976)	85 (32 – 114)	Tserendorj et al. (2022b)
Afsin, Turkey	Soil samples*, n = 21 (0–15 cm)	33 (7-78)	36 (26-49)	379 (304-744)	–	Cevik et al. (2008)
Ajka, Hungary	Soil samples*, n = 38 (undisturbed, 0–20 cm)	129 (15-883)	27 (12-43)	337 (146-596)	20 (3*[X] −150)	Papp et al. (2002)
Ajka, Hungary	Soil samples*, n = 47 (disturbed, 0–20 cm)	136 (21-1256)	25 (15-41)	329 (176-567)	17 (2-69)	Papp et al. (2002)
All over the country, India	Surface soil samples* n= >30	37 (14-155)	69 (18 - 155)	396 (11-706)	–	Mishra (2004)
Baoji, China	Soil samples*, n = 24 (0–25 cm)	32 (23-40)	50 (38-66)	720 (498-858)	–	Dai et al. (2007)
Barapukuria, Bangladesh	Soil samples*, n = 24 (0–10 cm)	103 (51-77)	103 (71-126)	494 (210-763)	–	Habib et al. (2019)
Figueira, Brazil	Soil samples*, n = 52 (0–25 cm)	151 (12-282)	39 (18-55)	233 (88-299)	–	Flues et al. (2002)
Kapar, Malaysia	Surface soil samples*, n = 14 (0–5 cm)	63 (31 - 152)	50 (20-74)	288 (194-358)	–	Amin et al. (2013)
Lodz, Poland	Surface soil samples*, n = 29 (undisturbed; 0–30 cm)	16 (7-21)	15 (9-20)	310 (221-434)	5 (1-15)	Bem et al. (2002)
Megalopolis basin, Greece	Surface soil samples*, n = 14 (0–5 cm)	45 (21-125)	32 (24-40)	337 (234-412)	80 (7-314)	Papaefthymiou et al. (2013)
Obrenovac, Serbia	Soil samples*, n = 30 (disturbed, 0–10 cm)	32 (19-49)	33 (14-55)	598 (372-833)	–	Tanić et al. (2016)
Sevilla, Spain	Surface soil samples*, n = 67 (undisturbed; 0–5 cm)	38 (13-67)	43 (15-68)	445 (97-790)	29 (3*[X]-209)	Charro et al., 2013
Mean value of the World soil	Soils	35 (17-60)	45 (11-64)	412 (140-850)	–	UNSCEAR (2010)

* Authors named their samples which partially cover of the depth of urban soil samples.
*[1] the number of samples are below the detection limit in this study.
*[X] the number of samples are below the detection limit.

measured in Salgótarján (UNSCEAR, 2010).

The mean value of surface soil samples in the vicinity of CFPP in India is richer in ^{232}Th (Mishra, 2004), moreover, in Bangladesh (Habib et al., 2019) and Malaysia (Amin et al., 2013) are richer in ^{232}Th and ^{226}Ra, whereas in Brazil (Flues et al., 2002) and Ajka (Hungary) (Papp et al., 2002) much higher concentrations of ^{226}Ra are found compared to urban soils in Salgótarján (Fig. 5; Table 3). In Ajka, certain disturbed surface soils have activity concentrations as high as 1256 Bq kg^{-1} (Papp et al., 2002). It was reported that the Cretaceous brown coal from Ajka contains U concentration of approximately 94–152 mg kg^{-1} (Szabó, 1992), whereas Miocene brown coal from Salgótarján contains only 1 mg kg^{-1} U (Salazar – Yanez et al., 2021), shedding light on the differences in the local geology (age of coal, coalification process) which increase the U concentration and as a result the ^{226}Ra activity concentration in its by-product, namely coal ash (Table 1).

In fact, all the mean ^{226}Ra activity concentrations of soils compared in the vicinity of CFPP, such as in Ajka (Hungary), Serbia, Spain, Turkey, China, India, Brazil, Greece, Malaysia and Bangladesh, are higher than those in Salgótarján (Table 3). Furthermore, the ^{232}Th activity concentration is only lower in Poland, whereas it is almost the same in Ajka, Brazil, Greece, Serbia and Turkey but higher in Bangladesh, China, India, Malaysia and Spain (Table 3).

Potassium-40 activity concentrations are lower in Poland, Brazil and Malaysia, the same in Ajka (Hungary), Greece, India and Turkey, whereas higher in China, Serbia and Spain (Table 3). The ^{137}Cs activity concentration is only lower in Poland and higher in all the other countries (Table 3). Overall, urban soils from Salgótarján contain lower or the same values of ^{226}Ra, ^{232}Th, ^{40}K and ^{137}Cs when compared to soils in the vicinity of other CFPP and those worldwide.

3.2.2. Attic dust

The activity concentrations of ^{226}Ra in samples of attic dust from Salgótarján vary from 12.0 ± 6.0 to 145.6 ± 8.3 (mean: 43.3 ± 4.6 Bq kg^{-1}), including two outliers, that is, 143.5 ± 8.1 (STN35AD – family house) and 145.6 ± 8.3 (STN18AD – family house) (Figs. 1, 4A; Tables 1-2). The ^{226}Ra activity concentration of one sample, namely STN15AD – family house (Fig. S2), fell below the detection limit of 0.9 Bq kg^{-1}, which also exhibited the lowest ^{232}Th activity concentration (Fig. S2; Table 1). The outliers are at least five times higher than all other values for the samples of urban soil and brown forest soil (Fig. 4A; Table 1). The ^{232}Th activity concentrations ranged from 8.0 ± 2.6 to 94.3 ± 9.6 with a mean of 34.0 ± 2.4 Bq kg^{-1}, including two outliers, the same samples as for ^{226}Ra, those are, STN18AD – family house and STN35AD – family house (Figs. 1, 4B; Tables 1-2).

Activity concentrations of ^{40}K (in Bq kg^{-1}) ranged from 309.2 ± 21.7 to 1382.3 ± 76.6 with a mean of 534.4 ± 39.1 Bq kg^{-1}, including one outlier of 1382.3 ± 77.6 Bq kg^{-1}, namely STN40AD – family house (Fig. 4C; Tables 1-2). The K_2O concentration of this outlying sample, that is, STN40AD, is also significantly elevated as previously discussed in Chapter 3.1, presumably due to the potassium fertilizer. The ^{137}Cs activity concentrations vary from 5.5 ± 0.9 to 169.8 ± 2.9 with a mean of 88.5 ± 5.1 Bq kg^{-1} (Fig. 4D; Tables 1-2).

Due to the absence of a worldwide long-lived natural radioactivity database for attic dust, our data were compared to the urban soils and coal ash from Salgótarján, the attic dust samples from two other Hungarian industrial cities, namely Ózd and Ajka, and the surface soil samples in the vicinity of the CFPP in Ajka, Hungary, as well as those in other countries (Figs. 4–5; Tables 2-3).

It can be seen from the boxplots that the ranges of ^{226}Ra, ^{232}Th, ^{40}K and ^{137}Cs activity concentrations of the attic dust samples are wider than for the urban soil (Fig. 4; Tables 1-2). Therefore, the activity concentrations of these radionuclides are more variable in attic dust samples than in urban soils. However, the ^{226}Ra, ^{232}Th and ^{40}K values contain outliers unlike the urban soil ones. The activity concentrations of ^{226}Ra, ^{40}K and ^{137}Cs in the attic dust samples are statistically significantly higher than in the urban soils in Salgótarján when comparing their medians (Fig. 4; Table 2). However, no statistically significant difference was observed in their ^{232}Th activity concentrations (Fig. 4; Table 2).

The two outliers in the ^{226}Ra and ^{232}Th activity concentrations of the attic dust samples (STN18AD – family house and STN35AD – family house), form a distinct subgroup with the coal ash sample in terms of the ^{226}Ra-^{232}Th-^{40}K triplot (Fig. 5; Table 1), suggesting a strong connection between these radionuclides and the by-product coal ash of the CFPP (Fig. S1B). This supports that coal ash can be considered as an anthropogenic component in the samples of our study, indicating their contamination levels. Furthermore, attic dust samples STN17AD – family house and STN32AD – family house (Fig. 1) also exhibit high ^{226}Ra and ^{232}Th activity concentrations (Fig. 5; Table 1), moreover, are the closest samples to this subgroup in terms of the ^{226}Ra-^{232}Th-^{40}K triplot (Fig. 5). These sampling sites are located in the elevated and open areas of the eastern and southern parts of the city (Fig. 1; Table 1). The prevalent wind direction is from the northwest which is capable of transporting particles to the south from the nearby CFPP as well as from the coal ash cone, Inászó slag dump and Kucsurd Hill (Fig. 1), however, not to the east. It is assumed that the local weather conditions are capable of changing the pathway of airborne dust materials, e.g., because of the presence of the valley stretching from the west to the east, which can alter the direction of the wind (Tserendorj et al., 2022a).

It is interesting that the ^{226}Ra activity concentration of the sample STN15AD – storeyed house fell below the detection limit but the U activity concentration was the third highest among the attic dust samples. Its ^{232}Th activity concentration and Th concentration are the lowest (Figs. S2A–B; Table 1).

Attic dust samples from other Hungarian industrialized cities, namely Ózd and Ajka, show different ^{226}Ra activity concentrations than those recorded in Salgótarján. In Ózd, the values ranged between 9.5 ± 2.7 and 63.3 ± 0.9 with a mean of 35.7 ± 3.3 Bq kg^{-1} (Tserendorj et al., 2022b), which are lower than those in attic dust from Salgótarján (Fig. 5; Table 3), suggesting a different pollution source in Ózd, e.g., smelter slag (Salazar-Yanez et al., 2021) because of the former iron and steel factory. On the other hand, in Ajka, these values ranged from 64.2 ± 5.0 to 587.7 ± 5.6 with a mean of 318.9 ± 53.7 Bq kg^{-1} (Tserendorj et al., 2022b), which are much higher than those from attic dust samples in Salgótarján (Fig. 5; Table 3). This must have been caused by the unusually high uranium concentration in the Ajka brown coal (Szabó, 1992) and the fact that coal was combusted in Salgótarján for a shorter period from 1891 to 1973 than in Ajka from 1872 to 1995 (Papp et al., 2002; Wirth et al., 2012).

The mean ^{137}Cs activity concentrations in attic dust samples from Salgótarján are ~15 times higher than those in urban soil samples (Fig. 4D; Tables 1-2). This indicates that the ^{137}Cs activity concentration in attic dust, which has remained undisturbed for decade, is high, therefore, is able to represent the long-term dynamic accumulation of material (Cizdziel and Hodge, 2000; Tserendorj et al., 2022a). In contrast, in an open environment like in urban soil, the dispersion of particles attached to mobile ^{137}Cs radionuclides probably migrated to depths greater than 15 cm, were washed away during natural processes, namely dissolution in water and precipitation (Ritchie and McHenry, 1990), or ^{137}Cs was mixed as a result of changes to the landscape, including the infilling of playgrounds, parks, etc.

In summary, the studied radionuclides exhibit much higher concentrations (except for ^{232}Th) and also higher degree of variability in the attic dust than in the urban soils in this study area. A connection between the ^{226}Ra and ^{232}Th activity concentrations in the attic dust and coal ash was revealed based on the triplot. By comparing this relationship with two other industrial areas with different pollution sources revealed that their activity concentrations in the attic dust depend on those in the pollution sourcesRegarding the ^{137}Cs activity concentration in attic dust versus that in urban soil, it is clear that attic dust can accumulate pollutants better than urban soil, therefore, attic dust is a useful material for studies on pollution.

3.2.3. Coal ash

The coal ash sample from the local coal ash cone in Pintértelep (Fig. 1, S1-A) exhibits higher ^{226}Ra and ^{232}Th activity concentrations of 91.1 ± 1.7 and 69.5 ± 3.3 Bg kg^{-1} than all the other studied samples, i.e. urban soil, brown forest soil and attic dust, except for the two outlying attic dust samples (STN18AD – family house and STN35AD – family house), (Fig. 4A and B; Table 1). The activity concentration of ^{40}K in the coal ash sample of 414.8 ± 8.9 Bq kg^{-1} is much lower than in the majority of attic dust samples, moreover, the ^{137}Cs activity concentration is the lowest among all the studied samples, that is: 0.09 ± 0.4 Bq kg^{-1} (Fig. 4D; Table 1).

Coal ash exhibits lower ^{226}Ra, ^{232}Th and ^{40}K activity concentrations than the average for coal ash in Hungary and even lower than those from other European countries, namely the Czech Republic, Germany, Poland, Romania and Slovakia (Table 4) (Trevisi et al., 2018). However, it can clearly be seen on the triplot (Fig. S3) that the ratio of these three radionuclides to each other in the coal ash from Salgótarján is similar to those in the aforementioned countries (Fig. S3; Table 4). As was seen earlier, the two outlying attic dust samples (STN18AD – family house and STN35AD – family house), (Fig. 5) strongly correspond to the average European coal ash (Table 4) (Trevisi et al., 2018). Accordingly, these two attic dust samples can be rather representative as a proxy in terms of the geochemical features of the original unweathered coal ash compared to the studied coal ash cone in Pintértelep (Fig. 1, S1-A; Table 4). The reduction in the activity concentrations in the coal ash from Salgótarján can be explained by the long period of exposure since the CFPP started operating in 1891 (Wirth et al., 2012) as well as strong chemical (rain) and physical (wind) weathering processes acting on the local coal ash cone (Figs. S1–A) as reported by Szabó et al. (2007) and Abbaszade et al. (2022).

3.2.4. Relationships between radionuclides

Prior to any hypothesis testing to compare the samples of attic dust and urban soil, distribution of the radionuclides normality was tested (Shapiro and Wilk, 1965; Reimann et al., 2008) (Table 2) to provide an in-depth analysis for further statistical treatment. The dataset of radionuclides in attic dust is non-normally distributed (^{226}Ra: $p < 0.00$, ^{232}Th: $p < 0.00$ and ^{40}K: $p < 0.00$; Table 2), except for the ^{137}Cs activity concentrations ($p = 0.18$; Table 2). In contrast, the whole dataset for the urban soil samples is normally distributed (^{226}Ra: $p < 0.47$, ^{232}Th: $p < 0.53$ and ^{40}K: $p < 0.98$; Table 2) with the exception of ^{137}Cs ($p < 0.00$; Table 2). Regarding the non-normal distribution of samples, a nonparametric Spearman's correlation (Schober and Schwarte, 2018) was used to check the linear correlation between the activity concentrations. Between ^{232}Th and ^{226}Ra and between ^{232}Th and ^{40}K in urban soil ($r = 0.75$, $p < 0.01$; $r = 0.4$, $p = 0.04$, respectively) as well as in attic dust samples ($r = 0.92$, $p < 0.01$; $r = 0.33$, $p = 0.05$, respectively), significant positive correlations were observed, indicating that the geological source of these natural radionuclides was common as pointed out by Navas et al. (2011) and Tanić et al. (2016), which in this case is the long-term use of local Miocene brown coal (Kercsmár et al., 2010) and 82 years of combustion at the local CFPP. The absence of any correlation between ^{226}Ra and ^{40}K reflects the differences in the origin and mobilization of both natural radionuclides (Navas et al., 2011). No correlation was observed between ^{226}Ra, ^{232}Th, ^{40}K and ^{137}Cs as a consequence of the Chernobyl NPP accident, which released ^{137}Cs into the environment (De Cort et al., 1998).

Table 4
The average activity concentrations (Bq kg^{-1}) of ^{226}Ra, ^{232}Th and ^{40}K in coal ash samples from some European countries (Trevisi et al., 2018) as well as of coal ash (CA) from Salgótarján. For the purpose of a comparison, the values of the two outlying attic dust samples, namely STN18AD and STN35AD, are also shown.

Countries	Number of samples	^{226}Ra	^{232}Th	^{40}K
Poland	1941	200	118	798
Czech Republic	1378	146	86	669
Greece	686	1046	56	400
Romania	179	219	116	595
Slovakia	226	123	76	769
Hungary	75	110	114	435
Germany	30	164	94	517
Slovenia	2	250	37	383
Salgótarján (this study)	1	91	69	414
STN18AD (this study)	1	145	83	708
STN35AD (this study)	1	143	94	649

3.3. Relationship between radionuclides in attic dust and urban soil as a function of the distance from the coal-fired power plant

Among the studied radionuclides, the decreasing activity concentrations of ^{226}Ra in attic dust and urban soil samples show a significant correlation as the distance from the CFPP increases (attic dust: $r = -0.4$, $p < 0.01$; urban soil: $r = -0.4$, $p = 0.05$) (Fig. 6A). Interestingly, a similar correlation is observed for the U activity concentration of attic dust as a function of the distance from the CFPP ($r = -0.5$, $p < 0.01$) (Fig. S4). Such a correlation is also true for ^{232}Th in attic dust ($r = 0.4$, $p < 0.01$) (Fig. 6B). No correlation was observed between the other radionuclides and elemental concentrations as the distance from the CFPP varied.

Furthermore, the lowest activity concentrations of ^{226}Ra and ^{232}Th were measured in the brown forest soil (Fig. 4A and B, 6A-B), which is the furthest sampling site from the CFPP (8100 m away) (Fig. 6A and B), supporting that brown forest soil is a strong natural geogenic component of all the studied samples as previously stated, which was also confirmed by Abbaszade et al. (2022) using Pb isotopes. The two outlying attic dust samples (STN18AD – family house and STN35AD – family house) located <1400 m from the CFPP, show the highest activity concentrations of ^{226}Ra and ^{232}Th (Fig. 6A and B). This confirms that these attic dust samples are considered to be a proxy of unweathered coal ash as discussed above. Accordingly, their corresponding urban soil samples STN21US – other (roadside) and STN29US – playground, also show slightly elevated activity concentrations of ^{226}Ra and ^{232}Th (Fig. 6A and B). Question raised whether the attic dust-urban soil pairs (Fig. 6A–B, S5; Table 1) shed light on any relationship between the two types of samples. The ratio of attic dust to urban soil in terms of ^{226}Ra and ^{232}Th in the 17 sample pairs (Fig. 7; Table 1) exhibits a strong positive relationship ($r = 0.73$; $p = <0.01$; Fig. 7). 76% (n = 13 from the 17 pairs) of the attic dust samples have higher ^{226}Ra activity concentrations than those of ^{232}Th (Table 1). These pairs ($n = 13$) exhibit the highest potential influence of the coal ash (Fig. 6A–B, S5; Table 1) and may also reflect the undisturbed attic area. Two low ratios, namely 0.7/0.4 for STN27AD/STN32US and 08/0.4 for STN10AD/STN13US (Fig. 7), are associated with pairs showing higher activity concentrations of ^{232}Th in urban soil samples than in corresponding attic dust ones (Table 1). These sampling sites are located further than 2700 m to the west of the CFPP. The ages of these two houses are significantly different (STN27AD and STN10AD family houses: 78 and 38 years old; Table 1). Moreover, at least the older one would have been expected to exhibit elevated ^{226}Ra activity concentrations, but the roof of the attic is not perfectly isolated, meaning deposited particles might be transported or reaccumulating processes may occur. The other two pairs (STN09AD/STN11US and STN25AD/STN23US), showing highly comparable ratios of attic dust and urban soil in terms of ^{226}Ra and ^{232}Th activity concentrations, are situated <4500 m to the north of the CFPP (Fig. 6A–B, 8; Table 1). The prevailing wind direction is from the northwest (Tserendorj et al., 2022a), which is not favorable as far as the transportation of by-products, i.e. coal ash, towards the north is concerned (Fig. 1). This suggests again that local weather conditions can change the pathway of airborne dust materials as concluded in our earlier study (Tserendorj et al., 2022) since the presence of valleys can alter particle deposition pathways. Furthermore, it is clear that the geochemical features of attic dust were preserved for decades undisturbed unlike the disturbed urban

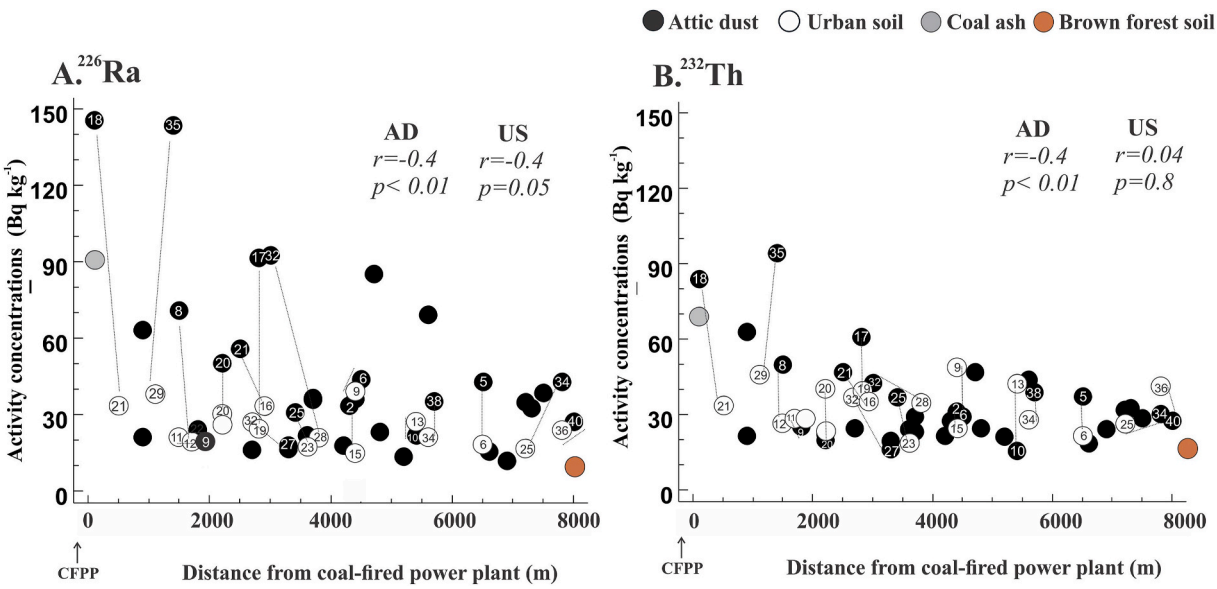

Fig. 6. The relationship between the distance of the sampling site from the coal-fired power plant (CFPP) and the activity concentrations of the studied radionuclides (A: ^{226}Ra, B: ^{232}Th). Note that sampling site STN15AD was excluded.

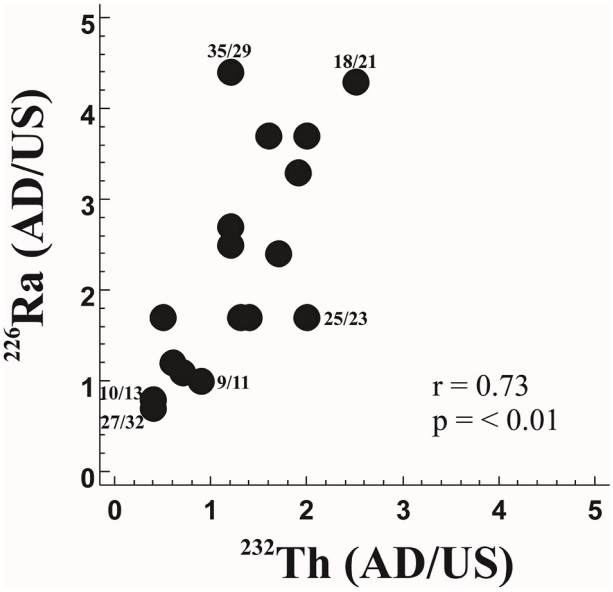

Fig. 7. The relationship between the ratios of samples of attic dust to urban soils with regard to the ^{226}Ra and ^{232}Th activity concentrations in attic dust-urban soil pairs (n = 17).

soil (Fig. 4A and B, 6A-B, 8A-B). Since the physical mechanisms of soil redistribution, namely deposition, and leaching/sorption processes in soil layers were in charge of controlling the dispersion of such radionuclides as ^{226}Ra and ^{232}Th (Navas et al., 2011).

3.4. Spatial distribution of the studied radionuclides in attic dust

Spatial maps, showing contours for identical radioactivity levels of the studied radionuclides, were calculated according to the Matheron algorithm (Matheron and Marie, 1965), which provides a meaningful estimation of spatial autocorrelation (Chilés and Delfiner, 2012) in the study area, including in areas where no data were available. The results for the ^{226}Ra and ^{232}Th activity concentrations, namely r^2 = 0.4 and 0.5, respectively, fitted models applicable for kriging (Cressie, 1990) to obtain interpolated activity concentration maps (Fig. 8A and B). The unusual STN15AD sample (Fig. 1, S2; Table 1) was excluded due to its unsatisfactorily high degree of variance compared to neighboring sites as previously described (Fig. 8A and B). Furthermore, inverse distance weighting (Lu and Wong, 2008) was performed to obtain an interpolated map of ^{40}K (Fig. S5) given its similar values of activity concentrations with regard to the data in the study area. For ^{137}Cs, the spatial autocorrelation has been published by Tserendorj et al. (2022a). Maps drawn for ^{226}Ra and ^{232}Th are highly similar to each other throughout the studied area (Fig. 8A and B). From the CFPP along lines I, II, III and IV, the same tendency in the activity concentrations of ^{226}Ra and ^{232}Th is seen (Fig. 8C). In other words, the closer the CFPP, the higher the activity concentrations of the radionuclides measured (Fig. 6A and B). Our observations support the findings of other studies, that elevated ^{226}Ra and ^{232}Th activity concentrations in soils are generally confined to no more than ~3000 m from the coal-fired power plants in Spain, China, Brazil and Serbia (Charro et al., 2013a, 2013b; Dai et al., 2007; Flues et al., 2002; Tanić et al., 2016). The attic dust dataset was the only one to provide the spatial distribution of the ^{226}Ra (Fig. 8A), ^{232}Th (Fig. 8B) and ^{40}K (Fig. S5) activity concentrations in the form of spatial maps.

3.5. Radiological dose assessment

To assess the risk the population living or working near the CFPP and slag dumps are exposed to (Fig. 1), the total absorbed gamma dose rate (D) [Eq. (1)] and the annual effective dose (E) [Eq. (2)] were calculated for the urban soil and attic dust samples. The total absorbed gamma dose rate (D) ranged between 35 and 64 nGy h^{-1} with a mean value of 48 nGy h^{-1} in urban soils from Salgótarján (Fig. 9A; Table S2), which is below the worldwide population weighted average value of D outdoors from terrestrial gamma radiation (59 nGy h^{-1}; range: 1–1200 nGy h^{-1}) and below the same values in Hungary (61 nGy h^{-1}, range: 15–130 nGy h^{-1}) (Fig. 9A) (UNSCEAR, 2010). Although the D value for all urban soils is higher than for the brown forest soil (32 nGy h^{-1}), it can be stated that the samples nearest to the CFPP (STN09US – park, STN20US – playground and STN29US – playground; Fig. 1), exhibit the highest D values of 64, 59 and 62 nGy h^{-1}, respectively (Table S2). Accordingly, the CFPP in Salgótarján and its slag dumps did not result in considerable amounts of radionuclides entering the urban soils.

Absorbed gamma dose rate (D) ranges between 22 and 155 nGy h^{-1} in attic dust samples with a higher mean of 74 nGy h^{-1} compared to

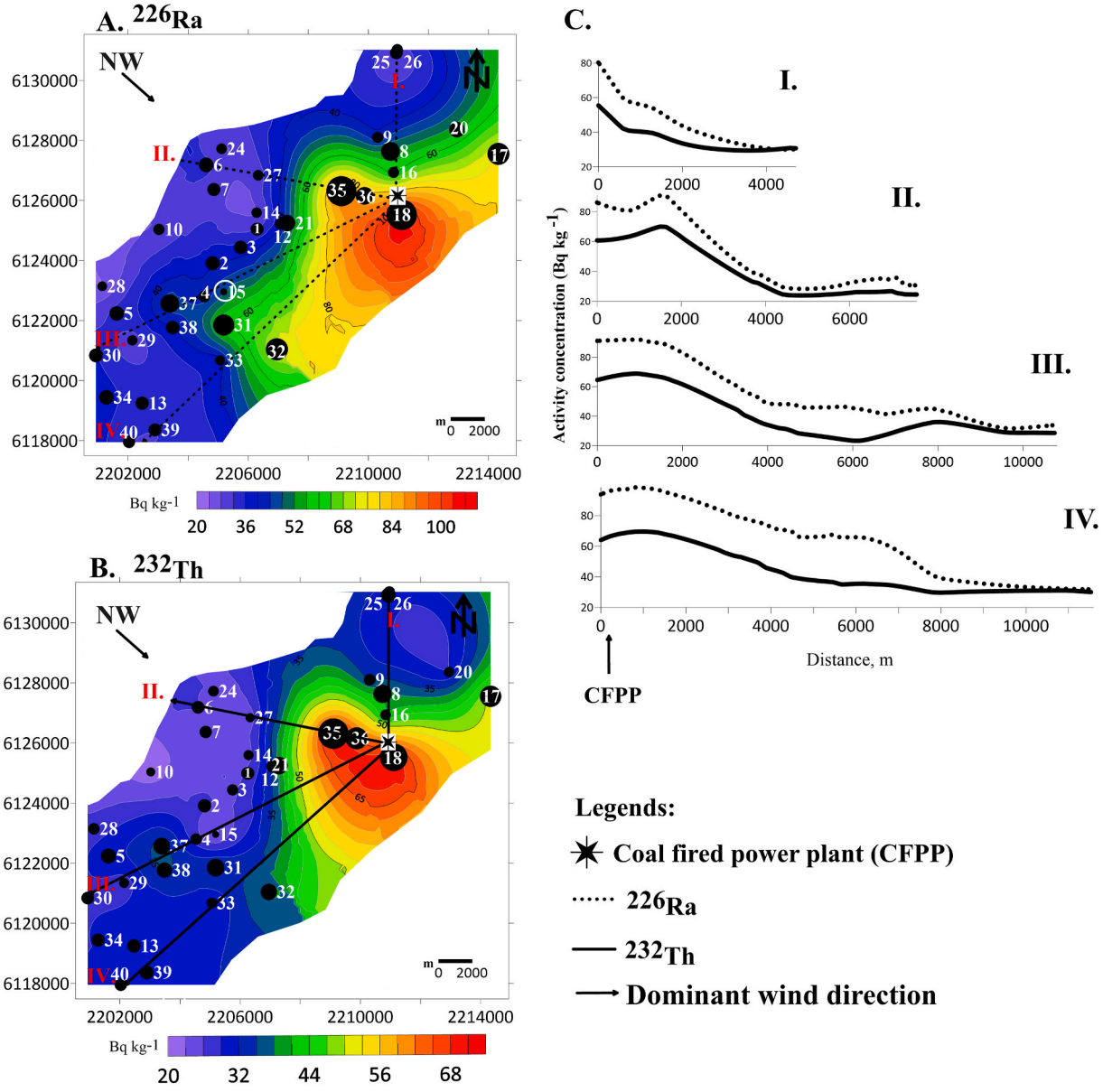

Fig. 8. The spatial distribution of ^{226}Ra (A) and ^{232}Th (B) in attic dust samples obtained by applying the ordinary kriging method. The size of the filled black circles is proportional to the activity concentrations of ^{226}Ra (A) and ^{232}Th (B). The black dashed lines in sections I to IV exhibit a decreasing trend (C) with regard to the activity concentrations of ^{226}Ra (A) and ^{232}Th (B) from sampling sites in the vicinity of the coal-fired power plant. The map is EPSG:3857 and WGS 84/Mercator projection (m).

urban soils (Fig. 9A; Table S2). Values of D for the coal ash is 101 nGy h^{-1}. In the absence of literature on attic dust, the calculated D values were compared to the worldwide population weighted average values concerning the absorbed dose rate in air inside dwellings (84 nGy h^{-1} with national averages ranging from 20 to 200 nGy h^{-1}) (UNSCEAR, 2010), which is rather consistent with the mean value of attic dust (74 nGy h^{-1}). Some of the attic dust samples and the coal ash have higher *D* values than the Hungarian average (95 nGy h^{-1}) but fall within its range (11–236 nGy h^{-1}) (Fig. 9A; Table S2). However, when exact radiological doses from attic dust are calculated, the fact that attic dust can cause doses in different ways to building materials must be taken into account, since it can move into dwellings in the form of dust and be inhaled or even ingested.

4. Summary

The elemental (U, Th, K and Cs) and activity (^{226}Ra, ^{232}Th, ^{40}K and ^{137}Cs) concentrations in urban soil samples in kindergartens, playgrounds, parks and others as well as those of attic dust found in family houses, churches, kindergartens and blockhouses were studied to identify the possible impact of contamination caused by former heavy industrial activity in the residential area of Salgótarján, Hungary.

The results showed that the elemental content of U, Th, K and Cs as well as the activity concentrations of ^{226}Ra, ^{232}Th, ^{40}K and ^{137}Cs in urban soil and attic dust are lower or equal to those in the literature in the vicinity of coal-fired power plant (CFPP) and soils worldwide. However, since the values for attic dust are higher than those for urban soils in Salgótarján, this study proved that attic dust provides an indirect assessment and serves as a highly sufficient historical record of local airborne dust deposition compared to the urban soil samples. Moreover, is an effective environmental media for monitoring the industrial urban environment in particular.

The elevated activity concentrations of ^{226}Ra and ^{232}Th in attic dust and urban soil from Salgótarján correspond to the close proximity of

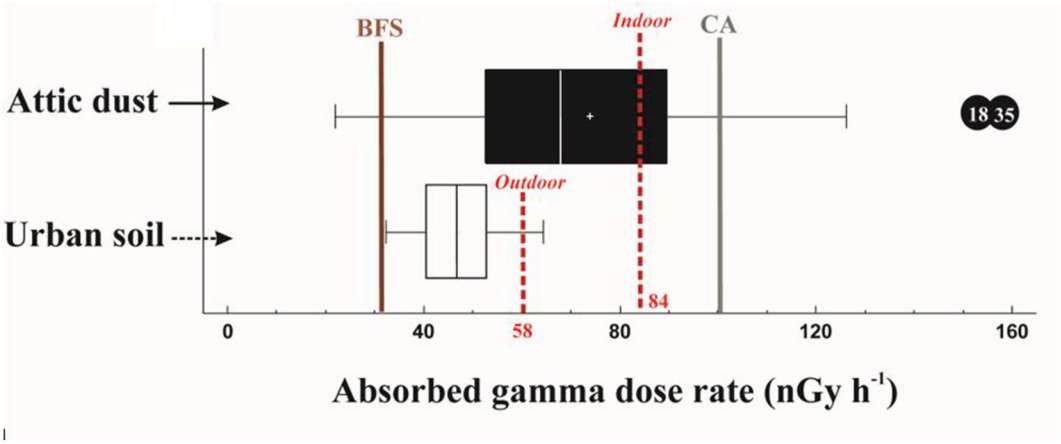

Fig. 9. Box and whisker plot of the calculated absorbed gamma dose rates (*D*) (nGy h^{-1}) all the studied samples, that is, 36 attic dust, 19 urban soils, 1 brown forest soil (BFS - denoted by a brown vertical line) and 1 coal ash (CA - denoted by a grey vertical line) from Salgótarján. The red dashed lines indicate outdoor and indoor worldwide average values for the absorbed dose rate (UNSCEAR, 2010). (For interpretation of the references to color in this figure legend, the reader is referred to the Web version of this article.)

sampling sites to the local CFPP. Spatial analysis confirmed that the closer the sampling site is to the CFPP, the higher the activity concentrations of the radionuclides observed. This indicates that the coal ash as a by-product of CFPP has a significant impact on residential areas in Salgótarján. Furthermore, attic dust and urban soil pairs shed light on their similar geochemical features.

The calculated total absorbed gamma dose rate (*D*) and annual effective dose (*E*) for urban soils indicate that the 82 years long operation of the CFPP in Salgótarján and different slag dumps do not cause increased levels of background radiation in city.

Our study recommends that a combination of U, Th, K and Cs content as well as activity concentration of ^{226}Ra, ^{232}Th, ^{40}K and ^{137}Cs radionuclides should be used to express the contamination source effectively.

Declaration of competing interest

The authors declare that they have no known competing financial interests or personal relationships that could have appeared to influence the work reported in this paper.

Data availability

Data will be made available on request.

5. Acknowledgements

This study was supported by the Stipendium Hungaricum Dissertation Scholarship Programme to DT. The authors are grateful for the residents for allowing them to enter their private properties, including attic areas, in order to collect attic dust and urban soil samples, thereby participating in this research. The cooperation of local authorities in Salgótarján is also appreciated who organized the collection of samples from kindergartens as well as of local church leaders who also provided historical and social background information. The authors would like to thank all of the LRG members for their help and kind-heartedness, particularly Áron Imre Bognár, Lívia Luczek, Boglárka Jaloveczki, Do Le Tan and Margit Kereskényi for their assistance with collecting and preparing the samples. This study was completed thanks to the cooperation of the Lithosphere Fluid Research Lab (LRG), Nuclear Security Department (NSD), Nuclear Analysis and Radiography Department (NARD) and Centre for Energy Research.

This is the 111th Publication of the Lithosphere Fluid Research Lab (LRG) at Eötvös Loránd University.

Appendix A. Supplementary data

Supplementary data to this article can be found online at https://doi.org/10.1016/j.jenvrad.2023.107291.

References

Abbaszade, G., Tserendorj, D., Salazar-Yanez, N., Zacháry, D., Völgyesi, P., Tóth, E., Szabó, Cs, 2022. Lead and stable lead isotopes as tracers of soil pollution and human health risk assessment in former industrial cities of Hungary. Appl. Geochem. https://doi.org/10.1016/j.apgeochem.2022.105397.

Ahmad, A.Y., Al-Ghouti, M.A., AlSadig, I., Abu-Dieyeh, M., 2019. Vertical distribution and radiological risk assessment of 137Cs and natural radionuclides in soil samples. Sci. Rep. 9 (1), 1–14. https://doi.org/10.1038/s41598-019-48500-x.

Alakangas, E., 2015. Quality Guidelines of Wood Fuels in Finland VTT-M-04712-15. 2015: Finland, p. 60. https://doi.org/10.13140/RG.2.1.3290.3127.

Alloway, Brain J., 2013. Heavy metals in soils. Handb. Toxicol. Met.: Fifth Edition 2, 885–936.

Amin, Y.M., Uddin Khandaker, M., Shyen, A.K.S., Mahat, R.H., Nor, R.M., Bradley, D.A., 2013. Radionuclide emissions from a coal-fired power plant. Appl. Radiat. Isot. 80, 109–116. https://doi.org/10.1016/j.apradiso.2013.06.014.

Antovic, N.M., Vukotic, P., Svrkota, N., Andrukhovich, S.K., 2012. Pu-239+240 and Cs-137 in Montenegro soil: their correlation and origin. J. Environ. Radioact. 110, 90–97. https://doi.org/10.1016/j.jenvrad.2012.02.001.

Balabanova, B., Stafilov, T., Šajn, R., Bačeva, K., 2011. Distribution of chemical elements in attic dust as reflection of their geogenic and anthropogenic sources in the vicinity of the copper mine and flotation plant. Arch. Environ. Contam. Toxicol. 61 (2), 173–184. https://doi.org/10.1007/s00244-010-9603-5.

Balabanova, B., Stafilov, T., Šajn, R., Tănăselia, C., 2017. Long-term geochemical evolution of lithogenic versus anthropogenic distribution of macro and trace elements in household attic dust. Arch. Environ. Contam. Toxicol. 72 (1), 88–107. https://doi.org/10.1007/s00244-016-0336-y.

Barba-Lobo, A., San Miguel, E.G., Lozano, R.L., Bolívar, J.P., 2021. A general methodology to determine natural radionuclides by well-type HPGe detectors. Measurement 181, 109561. https://doi.org/10.1016/j.measurement.2021.109561.

Bem, H., Wieczorkowski, P., Budzanowski, M., 2002. Evaluation of technologically enhanced natural radiation near the coal-fired power plants in the Lodz region of Poland. J. Environ. Radioact. 61 (2), 191–201. https://doi.org/10.1016/S0265-931X(01)00126-6.

Bihari, Z., Babolcsai, G., Bartholy, J., Ferenczi, Z., Kerényi, J.G., Haszpra, L., Ujváry, K. H., Kovács, T., Lakatos, M., Németh, A., Pongrácz, R., Putsay, M., Szabó, P., Szépszó, G., 2018. Éghajlat. Magyarország Nemzeti Atlasza: Természeti Környezet (Climate. National Atlas of Hungary: Natural Environment), pp. 58–69 (in Hungarian).

Canberra, 2000. Germanium well detector (WELL). Miron technologies. https://www.mirion.com/products/technologies/spectroscopy-scientific-analysis/gamma-spectroscopy/detectors/hpge-detectors-accessories/well-germanium-well-detector.

Cevik, U., Damla, N., Koz, B., Kaya, S., 2008. Radiological characterization around the Afsin-Elbistan coal-fired power plant in Turkey. Energy Fuel. 22 (1), 428–432. https://doi.org/10.1021/ef700374u.

Charro, E., Pardo, R., Peña, V., 2013a. Chemosphere Chemometric interpretation of vertical profiles of radionuclides in soils near a Spanish coal-fired power plant. Chemosphere 90 (2), 488–496. https://doi.org/10.1016/j.chemosphere.2012.08.008.

Charro, E., Pardo, R., Peña, V., 2013b. Statistical analysis of the spatial distribution of radionuclides in soils around a coal-fired power plant in Spain. J. Environ. Radioact. 124, 84–92. https://doi.org/10.1016/j.jenvrad.2013.04.011.
Chilés, J., Delfiner, P., 2012. In: Geostatistics: Modeling Spatial Uncertainty, second ed. Wiley, Canada. Cinelli.
Cinelli, G., De Cort, M., Tollefsen, T., 2019. In: European Atlas of Natural Radiation. Publication Office of the European Union, Luxembourg. https://doi.org/10.2760/520053.
Cizdziel, J.V., Hodge, V.F., 2000. Attics as archives for house infiltrating pollutants: trace elements and pesticides in attic dust and soil from southern Nevada and Utah. Microchem. J. 64 (1), 85–92.
Cizdziel, J.V., Hodge, V.F., Faller, S.H., 1998. Plutonium anomalies in attic dust and soils at locations surrounding the Nevada test site. Chemosphere 37 (6), 1157–1168. https://doi.org/10.1016/S0045-6535(98)00107-6.
Cizdziel, J.V., Hodge, V.F., Faller, S.H., 1999. Resolving Nevada test site and global fallout plutonium in attic dust and soils Using $^{137}Cs/^{239+240}Pu$ activity ratios. Health Phys. 77 (1), 67–75.
Coronas, M.V., Bavaresco, J., Rocha, J.A.V., Geller, A.M., Caramão, E.B., Rodrigues, M.L. K., Vargas, V.M.F., 2013. Attic dust assessment near a wood treatment plant: past air pollution and potential exposure. Ecotoxicol. Environ. Saf. 95, 153–160. https://doi.org/10.1016/j.ecoenv.2013.05.033.
Cressie, N., 1990. The origins of kriging. Math. Geol. 22 (3), 239–252.
Currie, L.A., 2004. Detection and quantification limits: basic concepts, international harmonization, and outstanding ("low-level") issues. Appl. Radiat. Isot. 61 (2–3), 145–149. https://doi.org/10.1016/j.apradiso.2004.03.036.
Dai, L., Wei, H., Wang, L., 2007. Spatial distribution and risk assessment of radionuclides in soils around a coal-fired power plant: a case study from the city of Baoji, China. Environ. Res. 104 (2), 201–208. https://doi.org/10.1016/j.envres.2006.11.005.
Dai, S., Seredin, V.V., Ward, C.R., Jiang, J., Hower, J.C., Song, X., Jiang, Y., Wang, X., Gornostaeva, T., Li, X., Liu, H., Zhao, L., Zhao, C., 2014. Composition and modes of occurrence of minerals and elements in coal combustion products derived from high-Ge coals. Int. J. Coal Geol. 121, 79–97. https://doi.org/10.1016/j.coal.2013.11.004.
Davis, J.J., Gulson, B.L., 2005. Ceiling (attic) dust: a "museum" of contamination and potential hazard. Environ. Res. 99 (2), 177–194. https://doi.org/10.1016/j.envres.2004.10.011.
De Cort, M., Dubois, G., Fridman, ShD., Germenchuk, M.G., Izrael, YuA., Janssens, A., Jones, A.R., Kelly, G.N., Kvasnikova, E.V., Matveenko, I.I., Nazarov, I.M., Pokumeiko, YuM., Sitak, V.A., Stukin, E.D., Tabachny, L.Ya, Tsaturov, YuS., Avdyushin, S.I., 1998. Atlas of Caesium 137 Deposition on Europe after the Chernobyl Accident. EUR-19801- EN-RU.
Demetriades, A., Birke, M., 2015. URBAN GEOCHEMICAL MAPPING MANUAL: Sampling, Sample Preparation, Laboratory Analysis, Quality Control Check, Statistical Processing and Map Plotting. EuroGeoSurveys, Brussels, Belguim.
Eisenbud, M., Petrow, H.G., 1964. Radioactivity in the atmospheric effluents of power plants that use fossil fuels. Science 144 (about), 288–289. https://doi.org/10.1126/science.144.3616.288.
EPA (Environmental Protection Agency), 2006. Technical Report on technologically enhanced naturally occurring radioactive materials from uranium mining volume 1 : mining and reclamation background. U . S . Environmental Protection Agency Office of Radiation and Indoor Air Radiation Protection Divisi 1 (2006), 1–225.
Finkelman, R.B., 1993. Trace and minor elements in coal. In: Engel, M.H., Macko, S. (Eds.), Organic Geochemistry. Plenum, New York, NY, USA, pp. 593–607.
Flues, M., Moraes, V., Mazzilli, B.P., 2002. The influence of a coal-fired power plant operation on radionuclide concentrations in soil. J. Environ. Radioact. 63 (3), 285–294. https://doi.org/10.1016/S0265-931X(02)00035-8.
Gabersek, M., Watts, M.J., Gosar, M., 2022. Attic dust: an archive of historical air contamination of the urban environment and potential hazard to health? J. Hazard Mater. 432 (November 2021), 128745 https://doi.org/10.1016/j.jhazmat.2022.128745.
Ghasemi, A., Zahediasl, S., 2012. Normality tests for statistical analysis: a guide for non-statisticians. Int. J. Endocrinol. Metabol. 10 (2), 486–489. https://doi.org/10.5812/ijem.3505.
Gosar, M., Šajn, R., Biester, H., 2006. Binding of mercury in soils and attic dust in the Idrija mercury mine area (Slovenia). Sci. Total Environ. 369 (1–3), 150–162. https://doi.org/10.1016/j.scitotenv.2006.05.006.
Habib, M.A., Basuki, T., Miyashita, S., Bekelesi, W., Nakashima, S., Phoungthong, K., Khan, R., Rashid, M.B., Reza, M.A., Islam, T., Techato, K., 2019. Distribution of naturally occurring radionuclides in soil around a coal-based power plant and their potential radiological risk assessment. Radiochim. Acta 107 (3), 243–259. https://doi.org/10.1515/ract-2018-3044.
Hatvani, I.G., Leuenberger, M., Kohán, B., Kern, Z., 2017. Geostatistical analysis and isoscape of ice core derived water stable isotope records in an Antarctic macro region. Polar Science 13, 23–32. https://doi.org/10.1016/j.polar.2017.04.001.
IAEA (International Atomic Energy Agency), 2003. Extent of Environmental Contamination by Naturally Occurring Radioactive Material (NORM) and Technological Options for Mitigation. Technical reports series No. 419).
Ilacqua, V., Freeman, N.C.J., Fagliano, J., Lioy, P.J., 2003. The historical record of air pollution as defined by attic dust. Atmos. Environ. 37 (17), 2379–2389. https://doi.org/10.1016/S1352-2310(03)00126-2.
Kercsmár, Z., Budai, T.G., Csillag, G.I., Selmeczi, I., Sztanó, O., 2010. Surface Geology of Hungary. Geological and Geophysical Institute of Hungary. Retrieved from. http://www.dnr.wa.gov/ResearchScience/Topics/GeosciencesData/Pages/gis_data.aspx.
Kis, Z., Völgyesi, P., Szabó, Zs, 2013. DÖME: revitalizing a low-background counting chamber and developing a radon-tight sample holder for gamma-ray spectroscopy measurements. J. Radioanal. Nucl. Chem. 298 (3), 2029–2035. https://doi.org/10.1007/s10967-013-2691-8.
Kovács, J., Tanos, P., Korponai, J., Kovácsné Székely, I., Gondár, K., Gondár-Sőregi, K., Hatvani, I.G., 2012. Analysis of water quality data for scientists. Water Quality Monitoring and Assessment. https://doi.org/10.5772/32173.
Laborie, J.M., Le Petit, G., Abt, D., Girard, M., 2000. Monte Carlo calculation of the efficiency calibration curve and coincidence-summing corrections in low-level gamma-ray spectrometry using well-type HPGe detectors. Appl. Radiat. Isot. 53 (1–2), 57–62. https://doi.org/10.1016/S0969-8043(00)00114-7.
Lauer, E.N., Hower, C.J., Hsu-Kim, H., Taggart, K.R., Vengosh, A., 2015. Naturally occurring radioactive materials in coals and coal combustion residuals in the United States. Environ. Sci. Technology journal. https://doi.org/10.1021/acs.est.5b01978.
Lioy, P.J., Freeman, N.C.G., Millette, J.R., 2002. Dust: a metric for use in residential and building exposure assessment and source characterization. Environ. Health Perspect. 110 (10), 969–983. https://doi.org/10.1289/ehp.02110969.
Llorens, J.F., 2001. Fernández-Turiel, J.L.; Querol, X. The fate of trace elements in a large coal-fired power plant. Environ. Geol. 40, 409–416. https://doi.org/10.1007/s002540000191.
Lu, G.Y., Wong, D.W., 2008. An adaptive inverse-distance weighting spatial interpolation technique. Comput. Geosci. 34 (9) https://doi.org/10.1016/j.cageo.2007.07.010.
Lu, X., Zhao, C., Chen, C., Liu, W., 2012. Radioactivity level of soil around Baqiao coal-fired power plant in China. Radiat. Phys. Chem. 81 (12), 1827–1832. https://doi.org/10.1016/j.radphyschem.2012.07.013.
Mann, H.B., Whitney, D.R., 1947. On a test of whether one of two random variables is stochastically larger than the other. Ann. Math. Stat. 18 (1), 50–60. https://doi.org/10.1214/aoms/1177730491.
Matheron, G., Marie, G.F.P., 1965. Les variables régionalisées et leur estimation: une application de la théorie de fonctions aléatoires aux sciences de la nature. Masson, Paris.
Mishra, U.C., 2004. Environmental impact of coal industry and thermal power plants in India. J. Environ. Radioact. 72 (1–2), 35–40. https://doi.org/10.1016/S0265-931X(03)00183-8.
Navas, A., Gaspar, L., López-Vicente, M., Machín, J., 2011. Spatial distribution of natural and arti fi cial radionuclides at the catchment scale (South Central Pyrenees). Radiat. Meas. 46 (2), 261–269. https://doi.org/10.1016/j.radmeas.2010.11.008.
Painecur, P., Muñoz, A., Tume, P., Melipichun, T., Ferraro, F.X., Roca, N., Bech, J., 2022. Distribution of potentially harmful elements in attic dust from the City of Coronel (Chile). Environ. Geochem. Health, 0123456789. https://doi.org/10.1007/s10653-021-01164-x.
Papaefthymiou, H.V., Manousakas, M., Fouskas, A., Siavalas, G., 2013. Spatial and vertical distribution and risk assessment of natural radionuclides in soils surrounding the lignite-fired power plants in megalopolis basin, Greece. Radiat. Protect. Dosim. 156 (1), 49–58. https://doi.org/10.1093/rpd/nct037.
Papp, Z., Dezső, Z., 2003. Estimate of the dose-increment due to outdoor exposure to gamma rays from uranium progeny deposited on the soil around a coal-fired power plant in Ajka town, Hungary. Health Phys. 84 (6), 709–717. https://doi.org/10.1097/00004032-200306000-00003.
Papp, Z., Dezső, Z., Daróczy, S., 2002. Significant radioactive contamination of soil around a coal-fired thermal power plant. J. Environ. Radioact. 59 (2), 191–205. https://doi.org/10.1016/S0265-931X(01)00071-6.
Parzentny, H.R., Róg, L., 2019. The role of mineral matter in concentrating Uranium and Thorium in Coal and combustion residues from power plants in Poland. Minerals 9, 13–15. https://doi.org/10.3390/min9050312.
Reimann, C., Filzmoser, P., Garrett, R.G., Dutter, R., 2008. Statistical Data Analysis Explained: Applied Environmental Statistics with R. John Wiley & Sons, Ltd.
Reimann, C., Demetriades, A., Eggen, O.A., Filzmoser, P., 2009. EuroGeoSurveys Geochemistry Expert Group The EuroGeoSurveys Geochemical Map- ping of Agricultural and Grazing Land Soils Project (GEMAS) e Evaluation of Quality Control Results of Aqua Regia Extraction Analysis 049, 92 Norges Geologiske Undersøkelse Repor.
Pouyat, Richard V., Trammell, Tara L.E, 2019. Chapter 10 - climate change and urban forest soils. In: Busse, Matt, Giardina, Christian P., Morris, Dave M., Page-Dumroese, Debbie S. (Eds.), Book of Developments in Soil Sciences, 36. Elsevier, pp. 189–211. https://doi.org/10.1016/B978-0-444-63998-1.00010-0.
Ritchie, J.C., McHenry, J.R., 1990. Application of radioactive fallout cesium-137 for measuring soil erosion and sediment accumulation rates and patterns: a review. J. Environ. Qual. 19, 215–233, 1990.
Rudnick, R.L., Gao, S., 2004. Composition of the continental crust. Treatise on Geochemistry 3, 1–64. Elsevier, Oxford.
Sajn, R., 2005. Using attic dust and soil for the separation of anthropogenic and geogenic elemental distributions in an old metallurgic area (Celje, Slovenia). Geochem. Explor. Environ. Anal. 5 (1), 59–67. https://doi.org/10.1144/1467-7873/03-050.
Salazar-Yanez, N., Abbaszade, G., Tserendorj, D., Völgyesi, P., Zacháry, D., Szabó, K.Zs, Szabó, Cs, 2021. Assessment of 15 Heavy Metals in Urban Soils of Former Industrial City (Salgótarján, Hungary), 88. 16th Carpathian Basin Conference for Environmental Sciences, 30th March - 1st April, Budapest, Hungary. 30th March - 1st April, Budapest Hungary. 88. https://www.researchgate.net/publication/358214503_XVI_KARPAT-MEDENCEI_KORNYEZETTUDOMANYI_KONFERENCIA.
Salminen, R., Batista, M.J., Bidovec, M., Demetriades, A., De Vivo, B., De Vos, W., Duris, M., Gilucis, A., Gregorauskiene, V., Halamic, J., Heitzmann, P., Lima, A., Jordan, G., Klaver, G., Klein, P., Lis, J., Locutura, J., Marsina, K., Mazreku, A., O'Connor, P.J., Olsson, S.A., Ottesen, R.T., Petersell, V., Plant, J.A., Reeder, S., Salpeteur, I., Sandström, H., Siewers, U., Steenfelt, A., Tarvainen, T., 2005. FOREGS Global Geochemical Baselines Programme. Geochemical Atlas of Europe. http://weppi.gtk.fi/publ/foregsatlas.

Schober, P., Schwarte, L.A., 2018. Correlation coefficients: appropriate use and interpretation. Anesth. Analg. 126 (5), 1763–1768. https://doi.org/10.1213/ANE.0000000000002864.

Shapiro, S.S., Wilk, M.B., 1965. An analysis of variance test for normality. No. 3/4 (Dec., 1965). Source: Biometrika, Dec., 1965 52, 591–611. Published by: Oxford University Press on behalf of Biometrika Trust Stable URL: https://www.jstor.org/stable/2333709.

Szabó, I., 1992. Measurements on environmental effects of sole emitted by the Ajka thermal power station. Fiz. Szle. 42, 55–63 (in Hungarian).

Szabó, M., Angyal, Zs, Szabó, Cs, Konc, Z., Marosvölgyi, K., 2007. Environmental effects of slag heaps from power station. Geogr. Rev. CXXXI (IV), 303–317 (in Hungarian with English abstract).

Tanić, M.N., Mandić, L.J.J., Gajić, B.A., Daković, M.Z., Dragović, S.D., Bačić, G.G., 2016. Natural radionuclides in soil profiles surrounding the largest coal-fired power plant in Serbia. Nucl. Technol. Radiat. Protect. 31 (3), 247–259. https://doi.org/10.2298/NTRP1603247T.

Trevisi, R., Leonardi, F., Risica, S., Nuccetelli, C., 2018. Updated database on natural radioactivity in building materials in Europe. J. Environ. Radioact. 187 (February), 90–105. https://doi.org/10.1016/j.jenvrad.2018.01.024.

Tserendorj, D., Szabó, K.Zs, Völgyesi, P., Nguyen, T.C., Hatvani, I.G., Jánosi, I.M., Abbaszade, G., Salazar-Yanez, Y.N., & Szabó, Cs Activity concentration of ^{137}Cs in undisturbed attic dust collected from Salgótarján and Ózd (northern Hungary) 252 (May). https://doi.org/10.1016/j.jenvrad.2022.106950.

Tserendorj, D., Szabó, K.Zs, Völgyesi, P., Nguyen, T.C., Abbaszade, G., Salazar-Yanez, N., Szabó, Cs, 2022. Determination of naturally occurring radionuclides in attic dust samples from different industrialized Hungarian cities using inductively coupled plasma mass spectrometry and gamma-spectroscopy. In: VIII Terrestrial Radioisotopes in Environment International Conference on Environmental Protection (TREICEP), October 4-7th 2022. Vonyarcvashegy, Hungary. Abstract Book, p. 34. https://doi.org/10.18428/TREICEP-2022.

Tukey, 1977. Exploratory Data Analysis. Communications in Computer and Information Science. https://doi.org/10.1007/978-3-662-45006-2_9.

UNSCEAR, 2010. Sources and Effects of Ionizing Radiation: United Nations Scientific Committee on the Effects of Atomic Radiation UNSCEAR 2008 Report, Volume I: SOURCES. Report to the General Assembly: Annex B. Exposures of the Public and Workers from Various Sources of Radiation. United Nations, New York. ISBN 978-92-1-142274-0.

Völgyesi, P., Jordan, G., Zacháry, D., Szabó, Cs, Bartha, A., Matschullat, J., 2014a. Attic dust reflects long-term airborne contamination of an industrial area: a case study from Ajka, Hungary. Appl. Geochem. 46, 19–29. https://doi.org/10.1016/j.apgeochem.2014.03.010.

Völgyesi, P., Kis, Z., Szabó, Zs, Szabó, Cs, 2014b. Using the 186-keV peak for ^{226}Ra activity concentration determination in Hungarian coal-slag samples by gamma-ray spectroscopy. J. Radioanal. Nucl. Chem. 302 (1), 375–383. https://doi.org/10.1007/s10967-014-3274-z.

Webster, R., Oliver, M.A., 2007. Geostatistics for Environmental Scientists, second ed. https://doi.org/10.1002/9780470517277

Wheeler, A.J., Jones, P.J., Reisen, F., Melody, ShM., Williamson, G., Strandberg, B., Hinwood, A., Almerud, P., Blizzard, L., Chappell, K., Fisher, G., Torre, P., Zosky, G. R., Cope, M., Johnston, F.H., 2020. Roof cavity dust as an exposure proxy for extreme air pollution events. Chemosphere 244, 125537. https://doi.org/10.1016/j.chemosphere.2019.125537.

Wirth, P., Černič Mali, B., Fischer, W., 2012. Using the potentials of post-mining regions - a good practice overview of central europe. Post-Mining Regions in Central Europe - Problems, Potencials, Possibilities, 269 pages. ISBN 978-3-86581-294-0.

Zacháry, D., Jordan, G., Völgyesi, P., Bartha, A., Szabó, Cs, 2015. Urban geochemical mapping for spatial risk assessment of multisource potentially toxic elements — a case study in the city of Ajka, Hungary. J. Geochem. Explor. 158, 186–200. https://doi.org/10.1016/j.gexplo.2015.07.015. ISSN 0375-6742.